MONTHLY NOTICES

OF THE

ROYAL ASTRONOMICAL SOCIETY

CONTAINING

PAPERS, ABSTRACTS OF PAPERS, AND REPORTS
OF THE PROCEEDINGS OF THE SOCIETY
1945

VOL. 105

Published and Sold by the
ROYAL ASTRONOMICAL SOCIETY
BURLINGTON HOUSE
LONDON, W. 1
1945

Price £1, 16*s*.

Printed in Great Britain by
NEILL & CO., LTD., EDINBURGH

MONTHLY NOTICES

OF THE

ROYAL ASTRONOMICAL SOCIETY

Vol. 105 No. 1

The Council elected the following as Fellows of the Society at the Council meeting on 1945 February 9:—

Ralph Stuart Atkinson, Beechwood, White Hill Avenue, Barnsley, Yorkshire;
Richard Beetham, M.A., 14 The Corners, Cleveleys, Blackpool, Lancashire;
Arthur Bernard Garnet Drabble, 116 Raleigh Street, Nottingham;
Gordon Glynne-Walton, White Lea Grange, Batley, Yorkshire;
Dudley Stewart Perfect, M.A., D.Phil., The Royal Observatory, Greenwich, London, S.E.10; and
Michael George Sumner, Woodbury, West Road, Bridport, Dorset.

The following candidates were proposed for election as Fellows of the Society, the names of the proposers from personal knowledge being appended:—

Josef C. Bartosik, D.S.C., Polish Naval H.Q., 51 New Cavendish Street, London, W. 1 (proposed by R. L. Waterfield);
John L. Hull, 15 Mount Stuart Road, North Hobart, Tasmania (proposed by T. L. MacDonald);
William Hugh Marshall, B.Sc., 83 Irvine Road, Kilmarnock, Ayrshire (proposed by W. M. Smart);
Arthur Herbert Prickett, F.R.Met.Soc., Deputy District Officer, H.M. Coastguard, Cromarty, Ross-shire (proposed by E. E. Perrin);
Raymond Frederick Saxe, B.Sc., 15 Rivington Avenue, Woodford Green, Essex (proposed by J. L. Haughton); and
Ernest Thomas Walcroft, M.I.Mar.E., 99 Brownlow Road, Horwich, near Bolton, Lancashire.

MEETING OF 1945 MARCH 9

Professor E. A. Milne, President, in the Chair

The President referred to the death of Sir Arthur Eddington, and read the following message of condolence which had been sent to Sir Arthur Eddington's sister (the Fellows standing):—

"Since the last meeting, the Council of the Royal Astronomical Society has heard with profound regret of the death of its Foreign Secretary, Sir Arthur Eddington, O.M., F.R.S. The Council begs to assure Miss Eddington of its deep sympathy with her in this unexpected bereavement, and shares to the utmost in her grief.

"The Council recalls that Sir Arthur Eddington served with distinction as President

during the years of the centenary celebrations of the Society. But more than this, it places on record its sense of the lustre which the scientific work of Sir Arthur Eddington has shed on the Society and on astronomy in general, and its appreciation of his inspiration and leadership. It regards with pride his achievements in so many different astronomical fields, and it recognizes that in him the Society has lost a thinker and investigator of genius, who enriched the sciences the Society especially promotes by his original and pioneering researches, as well as by the charm of his public writings and utterances. His memory will long remain fresh in the hearts and minds of Fellows of the Society."

The election by the Council of the following Fellows was duly confirmed:—

John Maurice Barnett, c/o Lloyds Bank Ltd., Woking, Surrey;
Cecil John Sidney Bromfield, Dingle Combe, Potters Cross, Iver Heath, Buckinghamshire;
George Edward Raven Deacon, D.Sc., F.R.S., Admiralty Research Laboratory, Teddington, Middlesex;
Frederick George Humphrey Elphick, 11A Broadway, Southall, Middlesex;
Cyril King, 12 Moorside South, Fenham, Newcastle-on-Tyne, 4;
Donald William Millar, B.Sc., 7 Bournville Road, Catford, London, S.E. 6;
William Daniel Morgan, 1764 St. Anthony Avenue, St. Paul, Minnesota, U.S.A.;
William Humphrey Robertson, B.Sc., Sydney Observatory, Sydney, N.S.W., Australia;
Frederico Rutllant, Trinity College, Cambridge; and
Carl Leo Stearns, Ph.D., Van Vleck Observatory, Wesleyan University, Middletown, Conn., U.S.A.

The following candidates were proposed for election as Fellows of the Society, the names of the proposers from personal knowledge being appended:—

William Parkinson Hirst, B.A., Longwood, Camp Ground Road, Newlands, Cape Town, S. Africa (proposed by J. Jackson);
Matthew Hall Lambert, 8 Lisle Road, South Shields, Durham (proposed by G. R. Goldsbrough); and
Hugh Percival Wilkins, 127 Eversley Avenue, Barnehurst, Kent (proposed by F. M. Holborn).

Ninety-five presents were announced as having been received since the last ordinary meeting, including:—

A. B. Woodward, *Considerations on the Substance of the Sun.* Facsimile reprint of original published Washington, 1801 (presented by the University of Michigan);
C. E. R. Bruce, *A new Approach in Astrophysics and Cosmogony* (presented by the author);
M. Davidson, *From Atoms to Stars* (presented by the author);
L. Goldberg and L. H. Aller, *Atoms, Stars and Nebulæ* (presented by the Committee for the continued Distribution of Astronomical Literature);
H. Spencer Jones, *The Atmosphere of the Planets* (presented by the author);
Scrap-book of the Transit of Venus Expedition to Kerguelen Island, 1874 (presented by Lt.-Colonel B. E. Coke); and
H. Shapley, *Galaxies* (presented by the Committee for the continued Distribution of Astronomical Literature).

The President announced that the Council had awarded the Gold Medal of the Society to Professor Bengt Edlén, Professor of Physics in the University of Lund, for his identification of the origin of the principal lines in the coronal spectrum.

MAGNETO-HYDRODYNAMIC WAVES AND SUNSPOTS

Hannes Alfvén

(Communicated by Professor B. Lindblad, Assoc.R.A.S.)

(Received 1944 December 13)

Summary

The difficulty of finding a mechanism by which sunspots could produce such strong magnetic fields as are always associated with them has led to a new theory of sunspots, according to which the magnetic field of the spot is the primary phenomenon. The other properties of a spot (*e.g.* the low temperature) are found to be due to the effect of the magnetic field on the solar atmosphere. As a spot magnetic field cannot be produced near the solar surface, it is supposed to originate near the Sun's centre and to be transmitted outwards along the magnetic lines of force of the Sun's general magnetic field in the form of a new type of wave, called the magneto-hydrodynamic wave. A brief survey of this theory is given in sections 1 and 2.

According to the theory the wave from a disturbance near the solar centre first reaches the solar surface at high latitudes and later proceeds towards the equator. As this explains the progression of the sunspot zone, it is of interest to compare the theory and observations in detail. Sunspot observations are therefore treated in order to derive a certain curve, the "sunspot zone progression curve", which shows the regular displacement of the spot zones (sections 3 and 4). Comparison of this curve with the theory permits some conclusions regarding the Sun's general magnetic field (sections 5–8).

A. *Introductory Remarks*

1. In a series of papers * a new theory of sunspots has been developed. The main features of this are the following.

Sunspots are always accompanied by strong magnetic fields. Many speculations have been made in order to explain this fact theoretically, but so far little success has been achieved in finding a mechanism capable of producing fields as strong as those observed. Even if a spot is considered as a whirl—which is dubious from the observational point of view—it cannot be understood how this whirl could give rise to the field. Elsasser's theory, which seems promising for the understanding of the general magnetic fields of the Sun and of the Earth, also fails when applied to sunspots.

It therefore seemed worth while to attempt another mode of approach to the sunspot problem. The existence of the magnetic field was postulated and its effect upon the solar atmosphere was investigated.†

It was shown that if there is a magnetic field **H** over a certain region of an electrically

* (1) H. Alfvén, "On the effect of a vertical magnetic field in a conducting atmosphere", *Ark. f. mat. astr. och fysik*, Bd. 29A, No. 11, 1943.

(2) "On the existence of electromagnetic-hydrodynamic waves", *ibid.*, 29B, No. 2, 1942. *Nature*, 150, p. 405, 1942.

(3) "On sunspots and the solar cycle", *ibid.*, 29A, No. 12, 1943.

(4) C. Walén, "On the theory of sunspots", *Ark. f. mat. astr. och fysik*, Bd. 30A, No. 15, 1944; Bd. 31B, No. 3, 1944.

† Alfvén, *loc. cit.* (1).

conducting atmosphere, the hydrostatic pressure within this region is decreased by the magnetostatic pressure $\mu H^2/8\pi$. If the hydrostatic pressure at a certain level is p_0 outside the magnetic field, the pressure p in the field region is

$$p = p_0 - H^2/8\pi,$$

assuming the permeability μ to be unity. This decrease in pressure can of course also be considered as an effect of the force $\mathbf{f} = (1/c)\mathbf{i} \times \mathbf{H}$ resulting from the magnetic field $\mathbf{H}$ and the current $\mathbf{i} = (c/4\pi)$ curl $\mathbf{H}$, which must flow in order to maintain the field. The pressure difference is quite considerable. If the field is 2000 gauss, for example, it amounts to $1{\cdot}6.10^5$ dynes cm.$^{-2}$.

The decrease in pressure explains the cooling of the spot. In fact, for hydrostatic equilibrium in the solar atmosphere it is necessary that the density of matter at a certain level be always the same. In the case of an ideal gas, the density of which is proportional to the pressure p and inversely proportional to the temperature T, this means that the temperature must be proportional to the pressure and consequently:

$$T = T_0(1 - H^2/8\pi p_0).$$

Hence a static equilibrium is possible only if the temperature in the magnetic field is lower than that outside it. Even if this temperature difference is once established, however, it must be smoothed out by radiation and conduction so that the hydrostatic equilibrium is disturbed. The result is an upward flow in the spot which causes an outward motion at the surface around the spot. In this way the cooling as well as the Evershed effect can be explained.

The fact that no sunspot without a magnetic field has been observed, nor any strong magnetic field without spots, favours this explanation.

When the properties of a sunspot had been found to be due to the existence of a magnetic field the next question arising was how this field is caused. This problem seems to be intimately connected with a new type of wave, tentatively called magneto-hydrodynamic waves.* Such waves can be produced in any electrically conducting liquid if a magnetic field $\mathbf{H}$ is given. Under these conditions a hydrodynamic motion of a certain volume with the velocity $\mathbf{v}$ gives rise to an electric polarisation

$$\mathbf{E} = (1/c)\mathbf{v} \times \mathbf{H}.$$

This electric field produces a system of currents $\mathbf{i}$, which interacts with the magnetic field so that mechanical forces are produced. In general these forces tend to slow down the volume elements initially in motion and accelerate volume elements in the neighbourhood. The result is that the initial state of motion is transferred to adjacent parts of the fluid, which later transfer the state of motion further on, thus causing a progressive wave.

The mathematical treatment of this phenomenon starts from the Maxwell equations:

$$\text{curl } \mathbf{H} = (4\pi/c)\mathbf{i}$$

$$\text{curl } \mathbf{E} = -\frac{1}{c}\frac{\partial \mathbf{B}}{\partial t},$$

together with

$$\mathbf{B} = \mu\mathbf{H}, \quad \mathbf{i} = \sigma(\mathbf{E} + \mathbf{v} \times \mathbf{B}/c),$$

and the hydrodynamic equation

$$\rho\frac{d\mathbf{v}}{dt} = \frac{1}{c}(\mathbf{i} \times \mathbf{B}) - \text{grad } p,$$

where ρ denotes the mass density, σ the conductivity and p the hydrostatic pressure.

* Alfvén, *loc. cit.* (2).

If the conductivity is infinite and the magnetic field **H** is composed of the given field H_0 (which is supposed to be homogeneous and directed along the z-axis of an orthogonal co-ordinate system) and a variable field H_y from the currents, it is easy to derive the equation of a plane wave from the above equations:

$$\frac{d^2H_y}{dt^2} = \frac{\mu H_0^2}{4\pi\rho}\frac{d^2H_y}{dz^2}.$$

This means that the velocity of the magneto-hydrodynamic wave is

$$V = H_0(\mu/4\pi\rho)^{\frac{1}{2}}.$$

The wave is characterized by a magnetic field H_y which in the case of a sine wave in the positive z-direction may be written (A = amplitude, ω = frequency)

$$H_y = A \sin \omega(t - z/V);$$

a hydrodynamic velocity,

$$v_y = -A(\mu/4\pi\rho)^{\frac{1}{2}} \sin \omega(t - z/V);$$

an electric current,

$$i_x = (Ac\omega/H_0)(\rho/4\pi\mu)^{\frac{1}{2}} \cos \omega(t - z/V);$$

and an electric field,

$$E_x = (AH_0/c)(\mu^3/4\pi\rho)^{\frac{1}{2}} \sin \omega(t - z/V);$$

and finally a pressure,

$$p = p_0 - (\mu A^2/8\pi) \sin^2 \omega(t - z/V).$$

The general case has been treated by Walén.* He has shown that any state of motion is transferred parallel and antiparallel to the given magnetic field H_0 with the velocity V. If the conductivity σ is not infinite, a kind of "diffusion" perpendicular to the field also takes place, but in the cases of interest in solar physics this effect is small and may probably be neglected. It is of special interest that he has considered the case when the waves are caused by an initial hydrodynamic whirl in the shape of a ring and shown that this ring is so split up that half of it travels in the direction of H_0 and half in the opposite direction. The two rings conserve their shape and move with the velocity V. Each ring is characterized by a hydrodynamic velocity v (in the plane of the ring) which is supposed to be constant inside the torus shell of the ring, and a magnetic field h which is parallel (or antiparallel) to v. The strength of h is

$$h = \pm H_0 v/V.$$

The kinetic energy $\rho v^2/2$ and the magnetic energy $\mu h^2/8\pi$ are always equal and the centrifugal force of the hydrodynamic motion v is exactly compensated by the stress of the magnetic lines of force of h. This means that the interaction with matter outside the ring is small.

2. The occurrence of sunspot-causing magnetic fields at the solar surface can be explained as due to magneto-hydrodynamic waves.† Suppose that the Sun's general field is a dipole field and that a hydrodynamic disturbance occurs at the centre (see Fig. 1A). This disturbance is transmitted as a wave along the magnetic lines of force with a velocity of the order of one metre per second. After about forty years it reaches the solar surface and causes strong magnetic fields there. The wave front first intersects the solar surface at high (northern and southern) latitudes, later proceeding towards the equator. This explains the wandering of the spot zone from high to low latitudes. The velocity of the spot zone is in reasonably good quantitative agreement with the theoretical velocity of the wave front.

Walén has shown that if the magneto-hydrodynamic waves are started by hydrodynamic whirls in the equatorial plane near the Sun's centre the characteristic magnetic

* *Loc. cit.*

† Alfvén, *loc. cit.* (3), and Walén, *loc. cit.*

polarities of sunspots can be explained.* He assumes that the solar magnetic field resembles the field from a circular current in the equatorial plane not too far from the

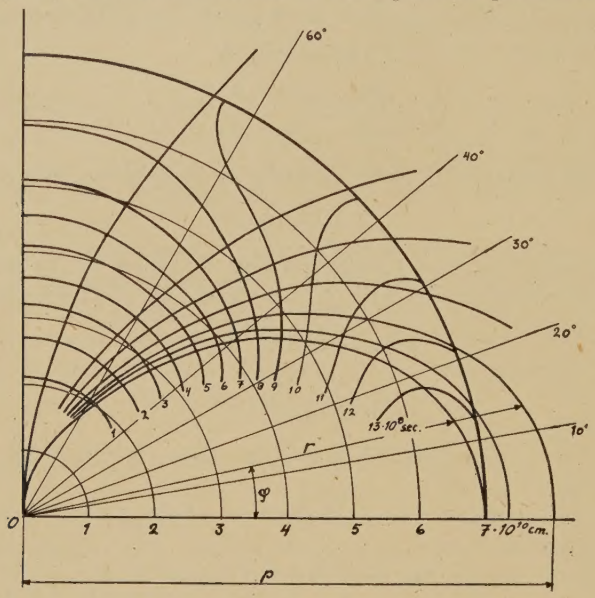

FIG. 1A.—*Magnetic lines of force and successive wave fronts calculated for the case of a dipole field (after Walén).*

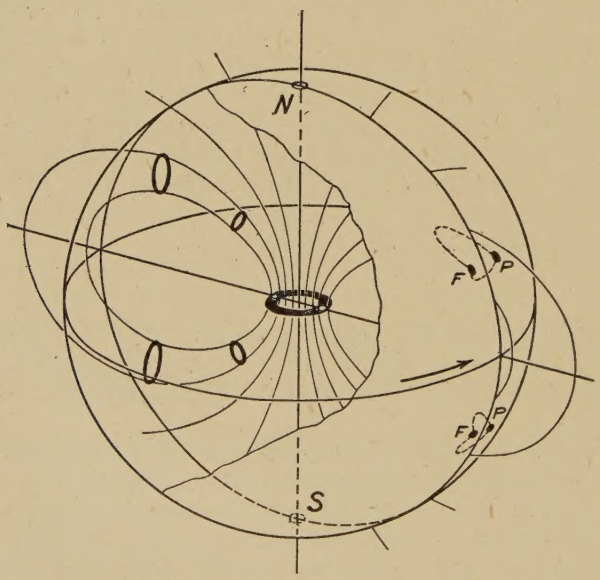

FIG. 1B.—*Whirl rings created near the Sun's centre travel along the magnetic lines of force to the surface where they produce bi-polar sunspots (after Walén).*

centre. Then the magnetic lines of force through the sunspot zone intersect the equatorial plane in a region near the Sun's centre (see Fig. 1B). If in this region a whirl ring with its plane coinciding with the equatorial plane occurs, it is split into two rings, one moving northward and the other southward along the magnetic lines of force. The magnetic whirl fields have opposite directions in these two rings. When they

* Walén, *loc. cit.*

finally reach and intersect the solar surface, magnetic fields occur at the two intersections between each ring and the surface, creating two spots with different polarities, which constitute the two components of a bipolar sunspot. Since the northern and the southern rings have magnetic fields with opposite directions, the polarities of the bipolar spots in the southern hemisphere are reversed with respect to the conditions in the northern hemisphere. In this way the remarkable law of the magnetic polarity of sunspots is explained.

The purpose of this paper is to give a further discussion of the relation between sunspots and the magneto-hydrodynamic waves and to try to interpret the sunspot observations in terms of the theory. In sections 3 and 4 the observations of sunspots are treated in order to derive the "sunspot zone progression curve", which shows the regular displacement of the sunspot zones towards the equator. In sections 5–8 this curve is compared with the theoretical curve for the progression of the magneto-hydrodynamic wave front. The possible conclusions are discussed regarding the shape and strength of the solar magnetic field.

B. *The Sunspot Zone Progression Curve*

3. According to the views summarized above, the wandering of the sunspot zones is due to the progression of the wave front of a magneto-hydrodynamic wave generated near the Sun's centre. In one of the cited papers * it was shown that the observed velocity of motion of the sunspot zone agreed reasonably well with the theoretical velocity of the wave front. However, the observational material was not in such a form as to make possible a more detailed comparison in this respect. For this reason we shall here subject the results of sunspot observations to further analysis.

According to the theory a sudden pulse at the Sun's centre (as earlier assuming the magnetic field to be an ideal dipole field) gives rise to a disturbance which becomes visible at the Sun's surface after a time $T(a)$, which is a function of the latitude a. Thus a single pulse would give rise to sunspots at a certain latitude only at the moment when the wave front reached the latitude in question. If we knew the time of the pulse at the centre and observed the time when the spots occurred at a certain latitude, we could find $T(a)$. As there seems to be no possibility of observing the time of a pulse at the centre, we can only hope to find the dependence upon the latitude of $T(a)$, but not its absolute value.

In reality, however, the problem is more difficult for there is always a series of pulses, constituting a sunspot cycle, which give rise to a lengthy series of spots at each latitude. In order to find the function $T(a)$ we might take a certain characteristic event of a sunspot period (at a certain latitude), *e.g.* its beginning, maximum, or end. None of these, however, is usually very well defined. We therefore prefer to take the centre of gravity

$$T_1(a) = \int t dS / \int dS \tag{B.1}$$

(S = spottedness as defined later) of the spots at a certain latitude as a measure of the time when the wave front reaches the latitude.

According to the theory the time of transit $T(a)$ is

$$T(a) = T_1(a) - T_0, \tag{B.2}$$

where T_0 is the time of the disturbance at the centre.

4. The function $T_1(a)$ can be derived from Spörer's observations.† As he has listed the sunspots observed, but not given their area, we write

$$T_1(a) = \Sigma tn / \Sigma n, \tag{B.3}$$

* Alfvén, *loc. cit.* (3).

† G. Spörer, "Beob. d. Sonnenflecken", I. *Publ. d. Astr. Gesellsch.*, XIII, Leipzig, 1874; II. *Fortsetzung d. Publ. d. Astr. Gesellsch.*, Leipzig, 1876; *Publ. d. Astrophys. Obs. Potsdam*, I (1879), 1881; IV, 1889; X, 1895.

where n is the number of spots at a certain latitude for each interval of time t. His tables were treated in the following way. Every sunspot which he denoted by a number or letter was listed with respect to the time and the latitude at which it first occurred. If a spot was observed at several rotations it was counted each time. The spots were grouped in intervals of 2° in latitudes and 5 solar rotations in time so that a "butterfly diagram" was obtained. In this diagram the borders between the different spot cycles were drawn. Near a minimum the spots at high latitudes were counted in the new cycle and those near the equator in the old cycle. In only a few cases could there be any doubt as to which of two adjacent cycles a spot should be counted in, but these spots do not affect the results appreciably.

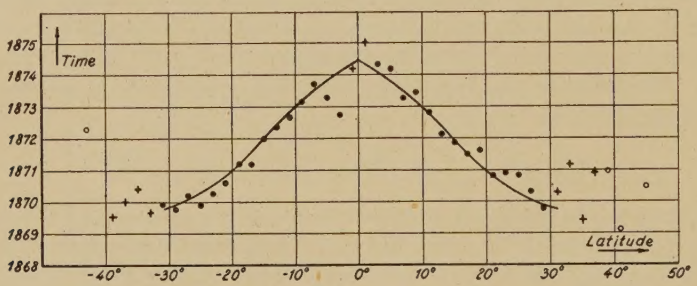

FIG. 2.—*Centre of gravity of sunspots at different latitudes according to Spörer's observations. Cycle* 11. *For comparison the average curve from Fig.* 7 *is drawn.*

● > 20 *spots.* + 5–20 *spots.* O 2–4 *spots.*

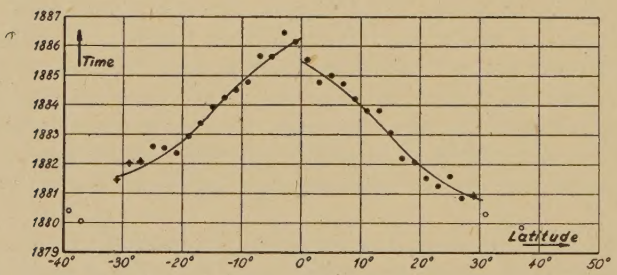

FIG. 3.—*Cycle* 12. *Spörer's observations.*

For the two cycles 11 (1866–1880) and 12 (1879–1890) the centre of gravity T_1 with respect to time has been calculated for every two degrees of latitude. The result is plotted in figs. 2 and 3. The curve obtained in this way will be called the *sunspot zone progression curve.*

In order to check the results obtained from Spörer's observations a similar analysis has been made using the results published in the "General Catalogue of Groups of Sunspots" from Greenwich.* In this catalogue, which comprises all sunspots lasting for two days or more, the columns "First seen, date", "Mean area corrected for foreshortening, whole spots", and "Mean position of group, latitude" were used. All spots for half-a-year occurring in every interval of 2° in latitude were grouped together and the sum of their total areas computed. A butterfly diagram was made showing the *spotted areas* as function of time (half-a-year groups) and latitude (two-degree groups). In the same manner as before $T_1(\alpha)$ was calculated. Fig. 4 shows the result for the cycle 16 (1923–1935).

* *Greenwich Observations*, 1911–1936.

The dots are situated more irregularly than in the earlier cases. This may be due to the fact that instead of counting the number of spots (as earlier) the spotted area was computed. In order to check this the Greenwich material was treated in the same way

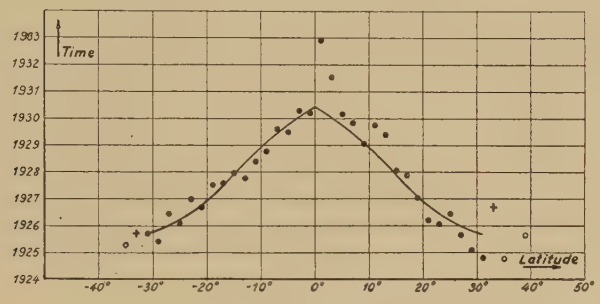

FIG. 4.—*Cycle* 16. *Greenwich observations. Average of spotted area taken.*

as Spörer's observations, so that a butterfly diagram was obtained, which shows the *number of spots* as a function of time and latitude (groups half-a-year and 2° in latitude). When $T_1(\alpha)$ was calculated from this diagram a more regular distribution was obtained,

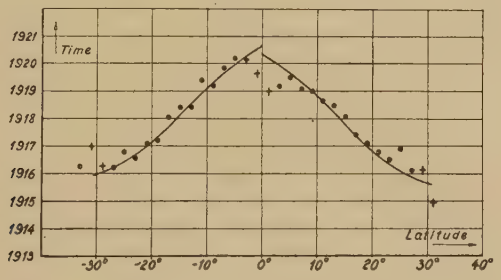

FIG. 5.—*Cycle* 15. *Greenwich observations. Average of number of spots taken.*

as shown in Fig. 6. This seems to be due to the fact that even one or two very big spots at the beginning or end of the cycle displace the centre of gravity considerably when the total surfaces are counted. It is thus preferable to use the number of spots and not the

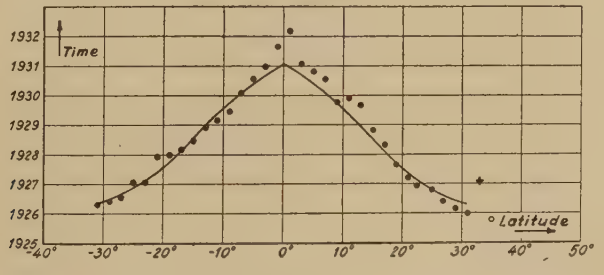

FIG. 6.—*Cycle* 16. *Greenwich observations. Average of number of spots taken.*

spotted area in deriving the sunspot progression curve. Moreover, this simplifies the numerical work.

The analysis of the Greenwich data has been extended to the cycle 15 (1911–1924). As the "General Catalogue" commences in the year 1916, the data for 1915 and earlier were taken from "Ledgers of areas and positions of groups of sunspots". Groups seen only on one day were not included. The result is plotted in Fig. 5.

The (unweighted) mean of the northern and southern hemispheres and all the four cycles analysed is shown in Fig. 7. The dots refer to the mean of the two cycles 11 and 12, the crosses to 15 and 16 (an arbitrary constant being added in order to make the absolute values coincide). The agreement between the first two and the second two cycles is rather remarkable. The smooth curve drawn in Fig. 7 will be used in future as the *observational sunspot zone progression curve.* The good agreement between the two series of observations gives the impression that it is determined with an error of only one- or two-tenths of a year.

For comparison this curve is superimposed upon the figures representing the individual cycles. For the cycles 12 and 15 the curve for the northern hemisphere is displaced somewhat with respect to that for the southern hemisphere, since there seems to be a systematic difference in time between the two hemispheres.

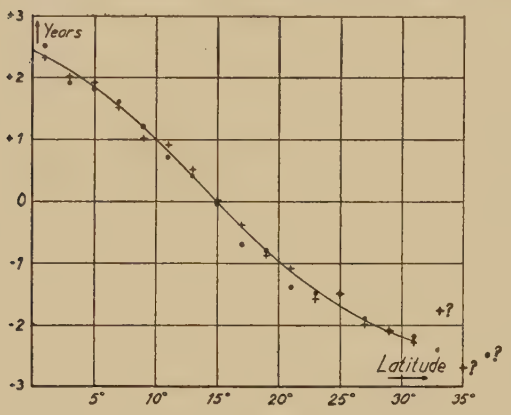

FIG. 7.—● *Mean of cycles* 11 *and* 12 *north and south.* + *Mean of cycles* 15 *and* 16 *north and south.*

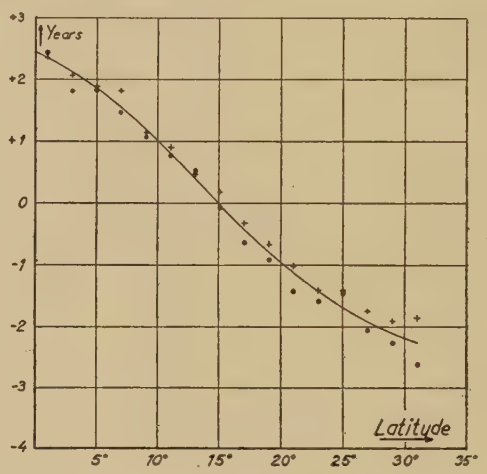

FIG. 8.—*Mean of cycles* 11, 12, 15 *and* 16. *North* ●. *South* +.

In Fig. 8 the means of all the four cycles for the two different hemispheres are represented. The curve may be a little steeper for the northern than for the southern hemisphere, but the difference is in any case only a few per cent.

It is of interest to note that the slope of the sunspot progression curve shows a velocity of 5°–10° per year, whereas the displacement of the mean latitude of the spots according to Waldmeier * varies between 1° and 5° per year.

C. *Theoretical Considerations*

5. We shall now discuss the sunspot zone progression curve from the theoretical point of view.

In one of the cited papers the time of transit from the centre to a certain latitude α at the Sun's surface was calculated under the assumption that the solar magnetic field is an ideal dipole field (*cf.* Fig. 1A).

The velocity V of the magneto-hydrodynamic waves is

$$V = H/\sqrt{4\pi\rho}, \tag{C.1}$$

where H is the magnetic field and ρ the mass density. (The permeability μ is supposed to be unity.) If H derives from a central dipole with moment a, we have

$$H = a/r^3 \sqrt{(1+3\sin^2\phi)}, \tag{C.2}$$

* M. Waldmeier, *Ergebnisse und Probleme der Sonnenforschung*, p. 127. Leipzig, 1941.

where r is the central distance and ϕ the latitude angle. The equation of a magnetic line of force is

$$r = p \cos^2 \phi, \tag{C.3}$$

where p is a parameter. The line element ds (in the direction of H) may be written

$$ds = \sqrt{(dr^2 + r^2 d\phi^2)} = p \cos \phi \sqrt{(1 + 3 \sin^2 \phi)} d\phi. \tag{C.4}$$

Thus we have

$$V = \frac{ds}{dt} = p \cos \phi \sqrt{(1 + 3 \sin^2 \phi)} \frac{d\phi}{dt} = \frac{a}{r^3} \frac{\sqrt{(1 + 3 \sin^2 \phi)}}{\sqrt{(4\pi\rho)}}. \tag{C.5}$$

After integration we find for the time of travel $T(\alpha)$ from the centre to a certain latitude α at the surface ($r = R_0$)

$$T(\alpha) = A \int_0^{R_0} \gamma \left(1 - \frac{r}{p}\right)^{-\frac{1}{2}} dr, \tag{C.6}$$

with

$$A = \pi^{\frac{1}{2}}/a, \tag{C.7}$$

$$\gamma = r^3 \rho^{\frac{1}{2}}, \tag{C.8}$$

$$p = R_0 \sec^2 \alpha. \tag{C.9}$$

The integration must be carried out numerically. For the comparison with the sunspot progression curve we do not need the absolute value of T but only its dependence on the latitude. As $T(0°) - T(90°)$ is small in comparison with $T(90°)$ it is inconvenient to compute $T(\alpha)$ and later take the differences. Hence we put

$$T(\alpha) = T(90°) + T''(\alpha) \tag{C.10}$$

and find

$$T'' = AF'', \tag{C.11}$$

where

$$F'' = \int_0^{R_0} \gamma X dr \tag{C.12}$$

and

$$X = \{1 - (r/R_0) \cos^2 \alpha\}^{-\frac{1}{2}} - 1. \tag{C.13}$$

As γ depends upon the mass density ρ, which is a function of r, we must know this function before we can compute F''. In a recent paper by G. Blanch, A. N. Lowan, R. E. Marshak, and H. A. Bethe * the density function is given. The values of F'' obtained through numerical integration using this function are denoted as F''_B. In order to ascertain how the results are affected by different assumptions regarding the density distribution, integrations have also been made using an older density function, given by Waldmeier † using the Lane-Emden polytrope $n = 3$. These values are denoted as F_W. The results of the integrations are given in the following table:—

α	F''_W	F''_B	F''_B/F''_W
°			
0	111·0	77·9	1·43
5		75·7	
10	102·6	71·8	1·43
15		65·8	
20	83·4	59·0	1·41
30	61·3	43·8	1·40
40	43·0	30·2	1·42
50	26·5	19·1	1·39
70	5·8	4·55	1·27

* *Ap. J.*, 94, 37, 1941. † *Loc. cit.*, p. 26.

The ratio F''_B/F''_W is remarkably constant. Indeed, for the latitudes of interest ($\alpha \leqslant 40°$) the ratio varies only by 2 per cent. Thus the differences between the solar models seem to affect only the absolute value and not the shape of $T''(\alpha)$. In the following we shall use the function F''_B (usually omitting the suffix B).

As sunspots are observed only in low latitudes (0°–40°), a comparison with observation must be restricted to this interval. It is convenient to refer the time when the sunspot progression curve reaches a certain latitude to a zero-point near the sunspot maximum. Hence we introduce

$$^{7\cdot0}F(\alpha) = F''(\alpha) - F''(15°) \qquad \text{(C.14)}$$

(where the index refers to the solar surface $R_0 = 7\cdot0 \cdot 10^{10}$ cm.).

This curve is plotted in Fig. 9.

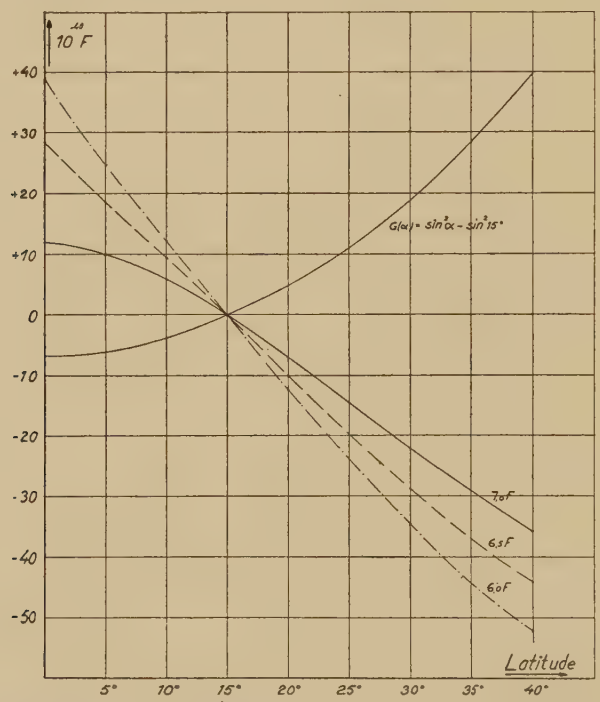

FIG. 9.—*Time when the wave front reaches different latitudes at the Sun's surface* ($^{7\cdot0}F$) *and at the depth* $0\cdot5.10^{10}$($^{6\cdot5}F$) *and* $1\cdot0.10^{10}$($^{6\cdot0}F$). *Ideal dipole field.*

6. The function $^{7\cdot0}F(\alpha)$ refers to the time when a disturbance reaches the solar surface. At first sight it is tempting to compare this function with the observational sunspot curve. This would be justified if the bipolar sunspots were small in comparison to the Sun's dimensions and no secondary phenomena occurred near the surface. The distance between the two spots of a bipolar sunspot, however, is frequently 10^{10} cm., which means that the magnetic ring producing the sunspots has about this diameter. As Walén * has shown, even the lowest part of the ring is of considerable importance to the sunspots fed by it, and this part may be $0\cdot5$–$1\cdot0 \cdot 10^{10}$ cm. below the solar surface when the spots occur. As the ring acts as a whole to a certain extent, it is not quite obvious whether the occurrence of sunspots should be referred to the time when the disturbance reaches the solar surface ($r = 7\cdot0 \cdot 10^{10}$ cm.) or, for example, the sphere $r = 6\cdot5 \cdot 10^{10}$ cm. or even $6\cdot0 \cdot 10^{10}$ cm.

It is therefore of interest to calculate the functions $^{6\cdot0}F(\alpha)$ and $^{6\cdot5}F(\alpha)$, which are

* *Loc. cit.*, § 13.

defined in the same way as $^{7\cdot0}F(\alpha)$ but refer to the surfaces $r=6\cdot0$ and $6\cdot5\,.\,10^{10}$ cm. instead of $r=7\cdot0\,.\,10^{10}$ cm. The calculations have been carried out numerically. The result is plotted in Fig. 9.

7. Up to now we have assumed the solar magnetic field to be an ideal dipole field. As such a field has an infinite strength at the centre, the real solar field must be different from this. The field is likely to be caused by currents in the Sun's interior (thermo-electric currents according to Elsasser) * which have a certain degree of symmetry with respect to the axis. The field is thus likely to be homogeneous in the neighbourhood of the centre. As we require a simple and yet physically reasonable model of the solar field, we assume it to be *a homogeneous field up to a certain central distance R_1 and a dipole field outside R_1*. This implies that we have assumed the currents responsible for the field to be concentrated to the spherical surface $r=R_1$ where they flow along the parallel circles, the current density being constant.

The pulse causing the magneto-hydrodynamic waves was initially assumed to occur

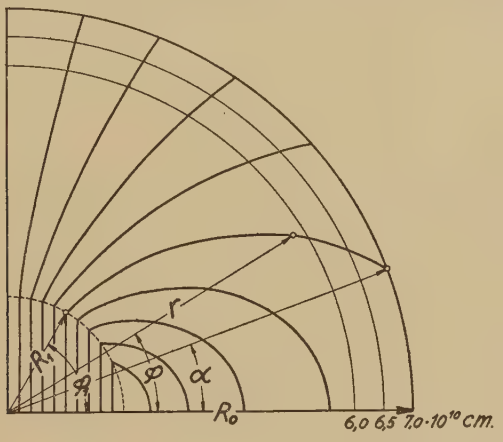

FIG. 10.—*Magnetic field according to assumption in section 7.*

at the Sun's centre. As we have now assumed the core to be homogeneous we must modify this assumption, because the lines of force which pass the sunspot zone do not pass the centre. The most simple assumption is that pulses occur in the equatorial plane simultaneously on all the lines of force. Then the sunspot progression curve is given by the time of travel from the equatorial plane to the solar surface (or, for example, the surface $R=6\cdot0$). As the observational curve was obtained by taking the centre of gravity of the spot cycle, we can also assume that the incipient pulses occur in an extended region symmetrical with respect to the equatorial plane, under the condition that the damping of the waves within this region is negligible. The essential point of our assumption is only that the pulses occur *simultaneously* (and symmetrically) on all the lines of force. Although we cannot be sure that the conditions for this are satisfied, it is a reasonable assumption upon which the subsequent reasoning is based.

7. We shall now investigate the effect of a core of homogeneous magnetic field. The time required by the wave to pass from the equatorial plane to the solar surface is

$$T=T_h+(R_0/R_1)T, \qquad \text{(C.16)}$$

where T_h is the time in the homogeneous magnetic field inside the sphere R_1 and $(R_0/R_1)T$ the time in the dipole field between R_1 and R_0.

A magnetic line of force intersecting the solar surface in latitude α reaches the sphere R_1 in latitude ϕ_1 given by (*cf.* Fig. 10)

$$\cos\phi_1=\sqrt{(R_1/R_0)}\cos\alpha. \qquad \text{(C.17)}$$

* W. M. Elsasser, *Phys. Rev.*, 55, 489, 1939.

In the homogeneous field

$$H = 2a/R_1^3, \tag{C.18}$$

it is parallel to the solar axis which we take as the z-axis. We find from (C.1) and (C.18)

$$T_h = \int \frac{dz}{V} = \frac{R_1^3 \pi^{\frac{1}{2}}}{a} \int_0^{\phi_1} r\rho^{\frac{1}{2}} \frac{d\phi}{\cos\phi}, \tag{C.19}$$

where ρ is a function of the central distance r. If the density falls as r^{-2} we have $r\rho^{\frac{1}{2}} = \text{const.}$ and find with the help of (C.17)

$$\frac{dT_h}{d\alpha} = \frac{dT_h}{d\phi_1}\frac{d\phi_1}{d\alpha} = \pi^{\frac{1}{2}} \frac{R_1^3}{a} \theta \left(\frac{R_0}{R_0 - R_1 \cos^2 \alpha} \right)^{\frac{1}{2}} \tan\alpha, \tag{C.20}$$

where

$$\theta = r\rho^{\frac{1}{2}} = \text{const.} \tag{C.21}$$

As R_1 is much smaller than R_0 we may consider the square root as approximately constant. Integrating and expanding $\log\cos\alpha$ into a series, we have approximately (for not too large values of α)

$$T_h = K + B\sin^2\alpha, \tag{C.22}$$

where K and B are constants.

If ρ is constant a similar calculation shows that T_h can be brought into the same form.

If we use the Blanch-Lowan-Marshak-Bethe density distribution, the integration must be carried out numerically. The results of such integrations for

$$R_1 = 1{\cdot}0,\ 1{\cdot}5,\ 2{\cdot}0,\ 2{\cdot}5,\ 3{\cdot}0 . 10^{10} \text{ cm.}$$

show that for $\alpha \leqslant 40°$

$$B = \frac{T_h(\alpha) - T_h(0)}{\sin^2\alpha} \tag{C.23}$$

is constant within about 5 per cent., so that we can still use the expression (C.22). Putting

$$B = \pi^{\frac{1}{2}} R_1^4 B_1/a \tag{C.24}$$

we have as a result of the numerical integrations

$10^{-10}R_1$	1·0	1·5	2·0	2·5	3·0
B_1	0·9	1·4	2·3	2·7	2·5

We have now to calculate the time (R_1 to R_0)T in the dipole field. As a dipole field is very strong near the dipole, the velocity of the magneto-hydrodynamic waves is very great. Thus the time from the centre to $r = 2.10^{10}$ cm. does not amount to more than 3–5 per cent. of the time out to the surface. Hence, if R_1 is not too large, we can approximately replace (R_1 to R_0)T by T which is calculated in section 5.

The result of numerical integrations of T_h and of (R_1 to 7·0)T (taking account also of the small difference between (R_1 to R_0)T and T) is given in Fig. 11.

According to our findings the theoretical sunspot progression curve in the case of a core of homogeneous magnetic field may be written

$$T(\alpha) - T(15°) = AF(\alpha) + BG(\alpha), \tag{C.25}$$

where

$$G(\alpha) = \sin^2\alpha - \sin^2 15° \tag{C.26}$$

and $A = \pi^{\frac{1}{2}}/a$ (a = dipole moment). B is given by (C.24), and $F(\alpha)$ stands for one of the functions represented in Fig. 9.

8. We shall now compare the theoretical result with the observational sunspot pro-

gression curve. If we take the curve $^{7\cdot0}F$ and add a suitable $\sin^2$-term, we can obtain approximately the S-shape exhibited by the observational curve. However, the tangent of the theoretical curve for $\alpha=0$ is horizontal, but the observational curve does not give the impression that it is becoming horizontal near the equator, although the values at very low latitudes are unreliable. If, instead, we take the $^{6\cdot5}F$ curve, this is almost a straight line. The difference between this and the observational curve may not be definitely outside the limits of error. The $^{6\cdot0}F$ curve cannot, with the addition of a positive $\sin^2$-term, be brought to agree with the observational curve.

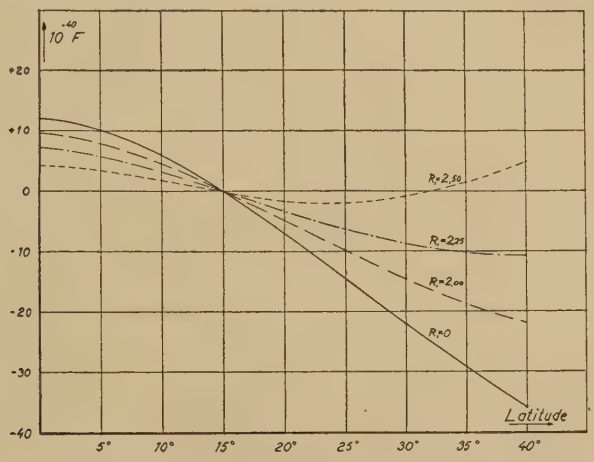

FIG. 11.—*Influence of a core (radius $=R_1$) of a homogeneous magnetic field. Time when the wave front reaches the solar surface.*

This shows that the function we have to use is intermediate between $^{7\cdot0}F$ and $^{6\cdot5}F$. The observational curve in Fig. 7 gives

$$T(0)-T(15)=2\cdot45 \text{ years}=7\cdot7\,.\,10^7 \text{ sec.}$$
$$T(15)-T(30)=2\cdot25 \text{ years}=7\cdot1\,.\,10^7 \text{ sec.}$$

Using these values we can calculate A and B from (C.25). We have

$$G(0°)=-0\cdot067;\quad G(30°)=0\cdot183.$$

Using $^{7\cdot0}F$ we have

$$F(0°)=12\cdot2\,.\,10^{40};\quad F(30°)=-22\cdot0\,.\,10^{40}.$$

This gives

$$A=1\cdot22\,.\,10^{-33};\quad B=108\,.\,10^7$$

and

$$a=1\cdot5\,.\,10^{33} \text{ gauss cm.}^3;\quad R_1=2\cdot4\,.\,10^{10} \text{ cm.}$$

Using $^{6\cdot5}F$ instead, we have

$$F(0°)=28\cdot4\,.\,10^{40};\quad F(30°)=-28\cdot6\,.\,10^{40}$$

and find

$$A=0\cdot28\,.\,10^{-33};\quad B=6\,.\,10^7.$$
$$a=6\cdot2\,.\,10^{33} \text{ gauss};\quad R_1=1\cdot8\,.\,10^{10} \text{ cm.}$$

In the latter case B is obtained as the difference between two almost equal figures so that a small change in the given values might make it zero or negative. Moreover, the values of B_1 in the table are correct only for $^{7\cdot0}F$, although the error is not large. Thus the latter value of R_1 is uncertain. (With $^{6\cdot0}F$ we would obtain $a=9\cdot2\,.\,10^{33}$; $B<0$.)

In Fig. 12 a comparison is made between the two theoretical curves corresponding to the above cases and the observational material used in Fig. 7. The figure indicates that the observational curve should be intermediate between the two theoretical curves, but perhaps more similar to the $^{7\cdot0}F$ curve than to the $^{6\cdot5}F$ curve.

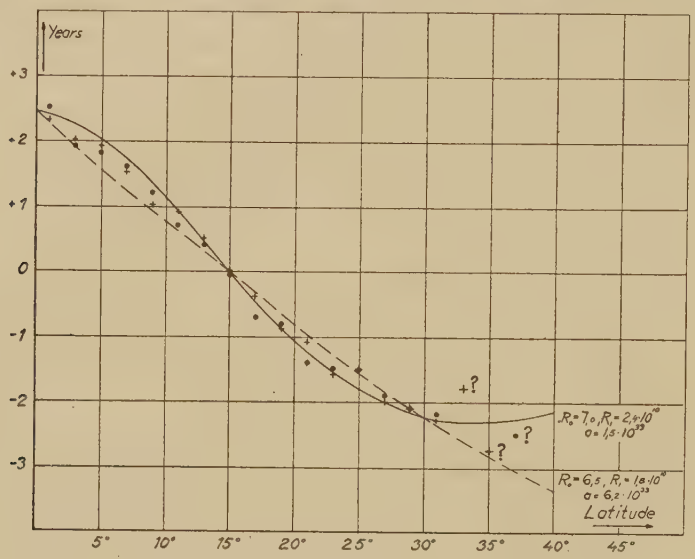

FIG. 12.—*Comparison between theoretical curves and observations.*

—— *Sunspots occur when the wave has reached the solar surface* ($7\cdot0.10^{10}$ *cm.*). *Homogeneous magnetic field within* $2\cdot4.10^{10}$ cm. *Dipole moment* $1\cdot5.10^{33}$ *gauss cm.*^{3}.

– – – *Sunspots occur when the wave has reached* $6\cdot5.10^{10}$ *cm. from the centre. Homogeneous magnetic field within* $1\cdot8.10^{10}$ *cm. Dipole moment* $6\cdot2.10^{33}$ *gauss cm.*^{3}. *Observational material from Fig.* 7.

If we confine ourselves to stating that the observational curve is intermediate between the two cases considered above we may conclude that

the Sun's magnetic dipole moment is between $1\cdot5.10^{33}$ *and* $6\cdot2.10^{33}$ *gauss cm.*^{3},

and further, that

the boundary between the dipole field and the homogeneous field lies within $2\cdot4.10^{10}$ *cm. from the centre.*

The first result is quite reasonable, for Zeeman effect measurements have given $4\cdot2.10^{33}$ gauss cm.^{3}, a value which is considered to be correct only within a factor of 2.* At first it was hoped that the study of the sunspot progression curve would make possible a more exact determination of the solar dipole moment, but—as we have seen—in view of the uncertainty regarding the phenomena close below the solar surface this cannot be realised at present. At all events it is satisfying that the value of the dipole moment falls within the expected range.

The second result implies that the currents responsible for the solar magnetic field are essentially situated inside 1/3 of the solar radius. This seems to be reasonable. According to Elsasser's theory we should expect the currents to flow at least not too far outside the Sun's convective core, which according to the stellar models is confined to about 1.10^{10} cm.

K. Tekniska Högskolan,
Stockholm:
1944 *October.*

* This corresponds to $H=25$ gauss at the pole, which is considered to be the most probable spectroscopic value. Compare Epstein, *Phys. Rev.*, 53, 862, 1938.

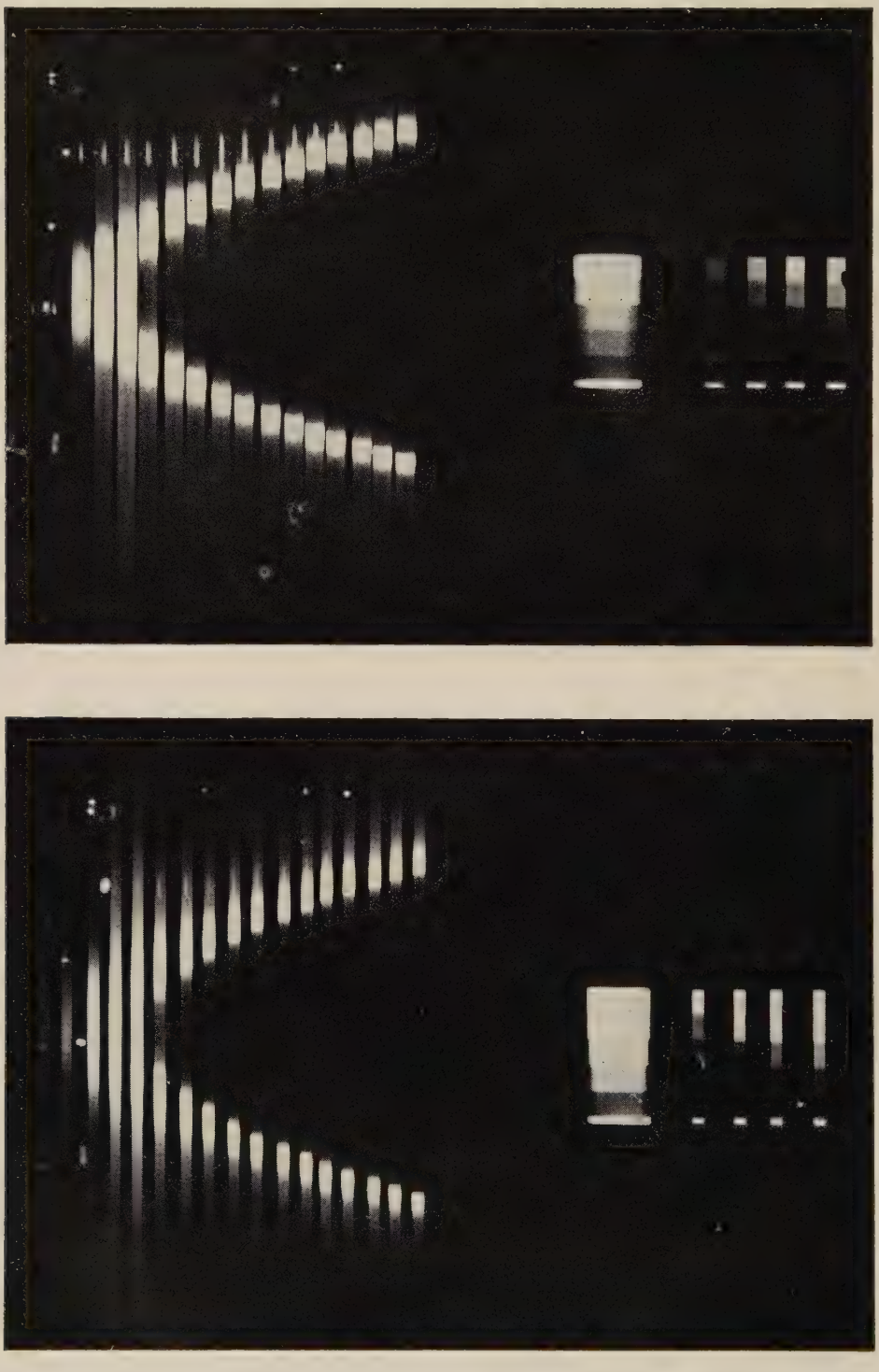

Spectra of two prominences showing the lines hydrogen $H\alpha$ in A and helium D_3 in B. The brighter prominence is visible on ten cuts, the fainter prominence on two. In this case the spectrum of the skylight is of considerable intensity, and $H\alpha$ can be seen in absorption. On the right there are spectra of the solar centre and exposures for the purpose of photometric calibration.

H. A. Brück and W. Moss, Intensities of hydrogen Hα and helium D_3 in Solar Prominences. Paper II.

INTENSITIES OF HYDROGEN *Hα* AND HELIUM D_3 IN SOLAR PROMINENCES. PAPER II

H. A. Brück and W. Moss

(Received 1945 March 9)

Summary

In continuance of former work, values of intensity are given of the lines hydrogen *Hα* and helium D_3 for various regions of 21 prominences. Results appear to confirm previous observations in the sense that variations in the relative intensity of *Hα* and D_3 can be explained as curve of growth effects. In particular cases variations of excitation appear as systematic deviations from the theoretical curve of growth. The observations are in agreement with a curve of growth for a temperature of 5000° as temperature of the solar boundary.

1. *Introduction.*—The present paper is a continuation of a study of line intensities in solar prominences which has been described in a previous paper *, in which also values of intensity of the lines hydrogen *Hα* and helium D_3 have been given for a number of points in 9 prominences. The chief result of Paper I, which may profitably be repeated here, was the observation that, in confirmation of earlier work by Minnaert and Slob †, variations of the intensity ratio $H\alpha/D_3$ can be explained by the effect of self-absorption on *Hα*, and that the observed rate of increase in the intensity of *Hα* with increasing number of emitting hydrogen atoms is consistent with the theoretical curve of growth for Doppler broadening at a temperature of 5000°. No indication of the presence of turbulent motions of hydrogen atoms, which would be equivalent to the observation of a higher kinetic temperature, has been observed. These results have been derived on the assumption that differences of excitation within one and the same prominence which might cause differences in the relative intensities of *Hα* and D_3 can be neglected in a first approximation, and that the intensity of D_3 can be taken as a measure of the optical thickness of a prominence in hydrogen. Differences of excitation between different prominences have been allowed for in the process of fitting together the various observations.

In Paper I use was made of only a small part of those observations of prominences which had been obtained with the spectroheliograph of the Solar Physics Observatory, Cambridge, mainly during the summer and autumn of 1943. A further investigation of the available material was to elucidate some of the problems encountered in the interpretation of the first batch of observations.

2. *Observations and Reduction.*—The present paper contains results of observations on 21 prominences, 5 of which had been partly studied in Paper I. It is based on a number of plates, taken between May and October 1943, which can be considered to be homogeneous as regards factors such as intensity of scattered skylight, atmospheric definition or general quality for photometric measurement.

In Paper I a description has been given of the observational procedure by which consecutive sections ("cuts") of prominences have been photographed (see Plate I). Pairs of simultaneous exposures have been taken of the spectral regions near *Hα* and D_3 with

* *M.N.*, **103**, 258, 1943. Hereafter called Paper I.

† *Pr. R. Ac. Sc. Amst.*, **33**, 65, 1930. See also Unsöld, *Physik der Sternatmosphären*, p. 409, 1938.

TABLE I

Intensities of Hα and D_3 in Various Regions of 21 Prominences
(expressed in units of 10^{-2} A. of the continuous Spectrum of the Solar Centre)

Prom.	Height	$I(H\alpha)$	$I(D_3)$	k
	"			
1	20	0·75	0·050	
	32	0·59	·040	
	39	1·76	·115	0·95
	45	1·95	·151	
	50	1·51	·134	
	53	0·54	·044	
2	14	1·63	0·141	
	21	1·00	·074	
	27	1·25	·076	0·95
	38	0·64	·045	
3	12	1·61	0·604	
	16	1·29	·336	1·58
	19	0·57	·150	
4 (*a*)	17	1·43	0·078	
	18	1·51	·084	0·85
	22	1·86	·119	
(*b*)	64	2·08	0·125	
	67	1·49	·084	
	71	1·98	·110	0·85
	79	2·19	·125	
	94	1·34	·072	
5 (*a*)	20	2·23	0·076	
	25	1·97	·064	0·55
	14	1·21	·034	
	20	1·66	·042	
(*b*)	35	1·62	0·038	
	43	0·41	·009	0·55
	45	1·79	·036	
(*c*)	121	6·60	0·064	0·1?
6	18	1·93	0·59	
	16	2·02	·47	
	21	2·58	·90	1·50
	14	1·65	·39	
	31	1·19	·29	
7	6	3·22	0·145	
	6	1·99	·070	0·72
	10	2·58	·126	
	23	1·42	·061	
8	18	3·18	0·107	
	26	4·29	·160	
	35	3·70	·140	0·60
	43	2·42	·082	
	52	1·43	·035	
9 (*a*)	7	3·47	0·27	
	10	3·23	·31	1·00
	23	3·46	·32	
(*b*)	51	1·66	0·09	0·8?
10	11	4·31	0·61	
	14	3·72	·57	1·20
	22	2·82	·32	
	18	3·56	·40	
11	12	2·48	0·10	
	12	4·42	·20	
	21	2·68	·11	0·70
	15	3·76	·16	
	15	2·48	·10	
12	32	5·8	0·20	
	40	5·9	·23	
	49	5·8	·20	0·50
	57	5·4	·14	
	66	3·4	·07	
13	15	7·8	0·20	
	36	6·8	·16	0·40
	55	5·6	·14	
	77	2·4	·04	
14 (*a*)	14	2·28	0·32	
	18	3·70	·57	
	20	3·70	·56	
	26	2·44	·41	
	13	2·83	·38	
	18	2·90	·37	1·25
	31	3·00	·38	
	13	6·65	·93	
	21	5·27	·72	
	33	4·30	·67	
	18	7·32	1·13	
	28	6·65	0·97	
(*b*)	46	3·00	0·30	
	46	4·80	·47	(1·00)
	37	5·05	·62	
	42	4·65	·40	
15 (*a*)	14	8·7	0·28	
	17	8·4	·29	0·40
	23	6·6	·14	
	34	6·3	·13	
(*b*)	11	7·1	0·17	0·40

TABLE I—*continued*

Prom.	Height	*I*(*Hα*)	*I*(D_3)	*k*	Prom.	Height	*I*(*Hα*)	*I*(D_3)	*k*
	"					"			
16	6	7·4	0·15		20 (*a*)	18	4·8	0·21	
	8	10·1	·24	0·37		18	5·4	0·23	
	8	7·7	·19			20	8·4	0·47	
	14	9·4	·25			25	15·9	1·28	0·75
						25	9·8	0·68	
						26	8·9	0·54	
17	16	7·3	0·23			28	9·5	0·58	
	17	7·5	·13						
	17	7·4	·13						
	17	7·6	·15		(*b*)	48	3·9	0·52	
	17	8·2	·22	0·40		48	5·0	·50	(1·15)
	17	7·2	·18			49	3·8	·43	
	15	8·2	·22						
	13	8·9	·38						
					(*c*)	79	2·1	0·40	
						79	3·3	·54	(1·25)
18	41	8·4	0·72			82	3·6	·43	
	37	9·5	0·87						
	32	12·2	1·20						
	27	10·2	0·90	0·90	21	33	23·2	0·45	
	15	11·2	0·98			37	21·4	·43	
	13	11·5	1·10			41	22·9	·45	
	14	12·5	0·95			45	22·9	·48	
						49	19·2	·39	
						54	15·4	·31	
19	25	8·2	0·24			58	15·4	·31	0·00
	32	9·4	·27			62	14·9	·29	
	44	10·0	·30			66	14·9	·27	
	50	11·5	·42			70	12·8	·19	
	68	12·4	·46	0·45		74	7·8	·070	
	80	13·4	·44			78	3·0	·021	
	99	11·8	·40						
	127	13·7	·54						

the two cameras of the spectroheliograph. The plates (Ilford Astra VIII and Ilford Thin Film Panchromatic) carry additional exposures for photometric calibration and spectra of the solar centre to which all measures of intensity have been referred. The photometric reduction of the present plates has been essentially the same as previously. The Cambridge microphotometer has been used for recording photographic densities, and in the determination of equivalent widths allowance has been made for the presence of spectra of skylight whose intensity varies with distance from the solar limb and on which emission lines of prominences are superimposed.

3. *Results.*—The results obtained are given in Table I, which contains in the third and fourth columns equivalent widths of *Hα* and D_3 expressed in units of 10^{-2} A. and referred to the intensity of the continuous spectrum of the solar centre near the lines. Intensities are given for 138 points in 21 prominences which are arranged in order of average intensity. Only prominences in which intensities could be measured at not less than three points have been included in Table I. The second column gives the apparent heights of the various points above the photosphere, expressed in seconds of arc, as they follow from the measured positions of the photometer slit with respect to the solar limb. Values under the heading *k* have the same meaning as in Paper I and will be discussed in connection with Fig. 1.

Four prominences were sufficiently extended in height to be studied with two or three

separate sets of consecutive cuts at different levels, which are distinguished in Table I by suffixes (*a*), (*b*) and (*c*). The same distinction has been made when only one single observation of intensities could be made at a point lying in a region outside the normal set.

Among the factors which determine the accidental errors of the given values of intensity, the influence of errors arising from possible wrong settings of the photometer slit in the case of $H\alpha$ or D_3 or from the photometric reduction has been tested by making various independent records and reductions of the same plates. It appears that on this account intensities in Table I should be accurate within about ± 10 per cent.

Apart from variations from prominence to prominence, relative intensities of $H\alpha$ and D_3 are seen to vary considerably within one and the same prominence. As had already been observed by Minnaert and Slob, and as has been stated in Paper I, intensity ratios $H\alpha/D_3$ are generally found to decrease with increasing intensity of helium, or in other words, the rate of increase in the intensity of $H\alpha$ is found to fall off with increasing intensity of the corresponding helium line. It is to be discussed how far the present observations on $H\alpha$, like those in Paper I, can be explained as curve of growth effects.

If we first assume that the intensity of D_3 is proportional to the optical thickness of a prominence in hydrogen as well as helium, that means, if as previously we neglect variations of excitation or composition within a prominence, the observed values of $I(H\alpha)$ can be plotted against those of $I(D_3)$ and the results compared with the theoretical curve of growth for $H\alpha$ which corresponds to the assumption of a certain temperature for the solar boundary.

In Fig. 1, theoretical curves of growth giving the dependence of $\log I(H\alpha)$ on the logarithm of the number of emitting hydrogen atoms have been drawn for the boundary temperature of radiative equilibrium of 5000° and for a kinetic temperature of 30,000° as it appears to follow for the chromosphere from Redman's * work on profiles of chromospheric lines. The straight line with unit slope represents the curve of growth for infinite temperature.

Assuming that the number of emitting hydrogen atoms can be represented by the intensity of D_3, corresponding values of $\log I(H\alpha)$ † and $\log I(D_3)$ have been plotted, separately for every prominence of Table I. Each set of points has been shifted parallel to the axis of abscissæ until the best fit with the theoretical curve is obtained. The amounts by which each group of points has to be shifted vary from prominence to prominence over a total range of 1·25 in $\log I(D_3)$; following Unsöld's ‡ notation, they are given under heading k in Table I. The zero-point of the scale of abscissæ has been chosen so as to make the value of k zero for prominence 21. Relative shifts between different prominences indicate variations in the relative numbers of emitting hydrogen and helium atoms caused by variations of excitation or possibly composition.

If we consider first how far the observed intensities are consistent with the curve of growth for the "normal" temperature of 5000°, or how far they indicate the existence of a higher kinetic temperature, observations on the prominences 19, 20 and 21 are the most important, as in their case only does the difference between the two hypothetical curves of growth become large enough to make such a distinction possible. These prominences are not quite so bright in $H\alpha$ as a prominence which was studied in Paper I and found to be particularly useful for this purpose. However, if we neglect the group of six points belonging to prominence 20 which lie well below the theoretical curve, present observations appear to confirm the earlier result that, within the errors of observation, they can be well represented by the curve of growth for 5000° and do not in themselves demand the assumption of a much higher temperature such as 30,000°.

* *M.N.*, 102, 140, 1942.

† As in Paper I, these have been referred first to the intensity of the continuous spectrum of the solar limb instead of that of the solar centre.

‡ *Loc. cit.*

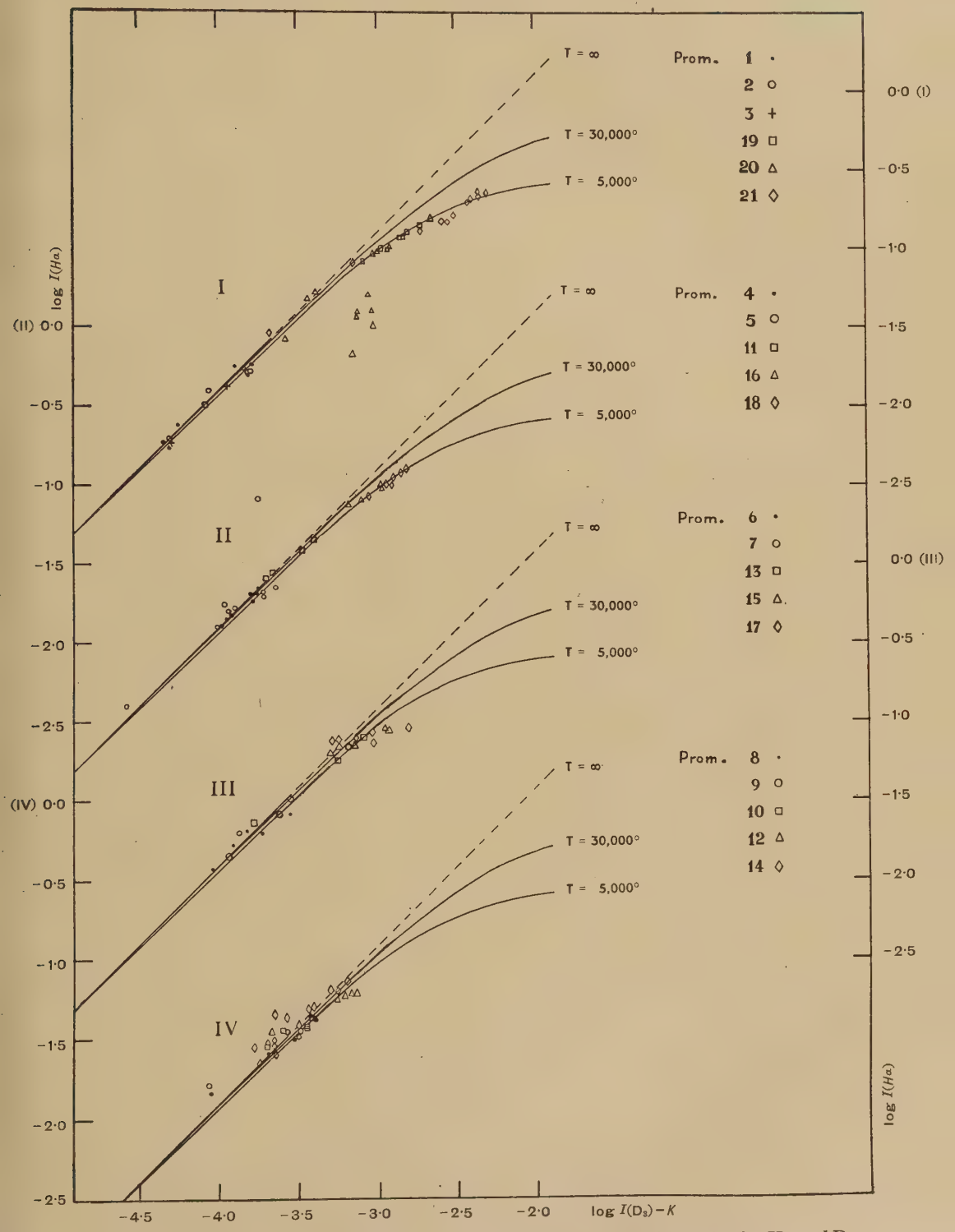

FIG. 1.—*Theoretical curves of growth for Hα, and observed values of intensity for Hα and* D_3 *in 21 prominences.*

This is true in the case of all three prominences, two of which show large-scale motion in the line of sight.

The group of six points which we have neglected so far corresponds to observations of the regions (*b*) and (*c*) of prominence 20, both of which are at a higher average level than points in 20 (*a*). If those six points are to fall on the theoretical curve, values of k of the order of 1·2 (put in brackets in Table I) instead of 0·75 have to be adopted. Since the corresponding observations are as accurate as those in region (*a*) which lie well on the curve, differences of excitation at the higher levels of (*b*) and (*c*) appear to be indicated in this manner, similarly as in the case of at least one of the prominences studied previously.

In the plots of II, III and IV of Fig. 1 a distinction between the curves of growth for $T = 5000°$ and $T = 30{,}000°$ becomes increasingly impossible, and the corresponding prominences therefore do not contribute anything to the question of the temperature of the solar boundary.

Regarding variations of excitation within one and the same prominence, there appears to be some more evidence for such a variation in the case of prominence 5 (*c*), where the deviation of the observed intensities from the theoretical curve on the assumption of a value of $k = 0{\cdot}55$ is considerably too great to be explained by errors of observation. However, as only a single point is concerned here, the value of k necessary to make it fall on the theoretical curve has been queried in Table I in this case as in the similar case of prominence 9 (*a*). Smaller but probably real differences of k are observed also between the regions (*a*) and (*b*) of prominence 14.

The observations on prominence 17 and to a less extent those on prominences 12 and 15 can be represented best by a straight line with slope less than unity. A similar observation was made in Paper I, and also by Unsöld in his reduction of Minnaert and Slob's observations. It appears to be real at least in the case of prominence 17 and to be another indication of varying excitation.

In the autumn of 1944 a pair of plates of excellent quality was obtained which shows a prominence of considerable extension both in height and in position-angle. This prominence can be studied on over twenty consecutive cuts at altogether more than a hundred points. It is hoped that the reduction of these spectra, which will be published in a separate paper, will contribute to elucidating the question of variations of excitation within one and the same prominence. The intensity distribution within this prominence or its structure in the light of *Hα* and D_3 will be given by sets of isophotes.

Solar Physics Observatory,
Cambridge:
1945 *March* 9.

ON THE INTEGRATION OF THE EQUATIONS DETERMINING THE STRUCTURE OF A STAR

F. Hoyle

(Received 1945 January 17)

Summary

A method is given whereby the equations determining the structure of a star can be integrated inwards from a point near the surface to the centre. The consistency of the method is established by using Cowling's solution, which was obtained from outward integration * (for the case of zero radiation pressure, uniform chemical composition, and Kramers' opacity formula).

---

1. *Introduction.*—The equations determining the structure of the stars have been solved in a few special cases by very tedious numerical computation. The difficulty in the computations arises because it has hitherto only been possible to carry the integration outwards from the centre to the surface of the star, and small errors in the computations occurring near the centre are found to lead to very large errors near the surface. It is clear that the labour of computation can be made very much lighter if a consistent system of integration inwards from the surface to the centre can be formulated, since in this case small errors in the numerical work will not seriously affect the run of the solutions. The object of the present paper is to provide such a method of inward integration. The method is applied explicitly to the case of a star of uniform chemical composition in which radiation pressure is negligible and the opacity is given by Kramers' law, for in this case the consistency of the method can be immediately established since the relevant computations are already available from outward integration. Similar investigations can be made for other cases, such as non-zero radiation pressure, stars of non-uniform composition, etc.

2. The equations of stellar structure for the case in which the opacity is given by Kramers' law, radiation pressure is neglected, and the energy generation is given by $E\bar{\rho}^2\bar{T}^\eta$ ergs per cm.^{3} per sec., where η is a constant of order 15, and $\bar{\rho}$, $\bar{T}$ are the density and temperature in c.g.s. units, are as follows:—

$$\frac{d}{dr}\frac{\mathfrak{R}\bar{\rho}\bar{T}}{\mu} = -\frac{G\bar{\rho}\bar{M}}{r^2}, \tag{1}$$

$$\frac{d\bar{M}}{dr} = 4\pi r^2\bar{\rho}, \tag{2}$$

$$L(r) = 4\pi E\int_0^r r^2\bar{\rho}^2\bar{T}^\eta dr, \tag{3}$$

together with

$$\bar{\rho}(r)/\bar{\rho}(0) = \{\bar{T}(r)/\bar{T}(0)\}^{1/(\gamma-1)} \tag{4}$$

inside the convective core (γ the ratio of specific heats is regarded as a constant throughout the convective core), and

$$\frac{1}{3}ac\frac{d\bar{T}^4}{dr} = -\frac{\bar{\alpha}(1-X^2)\bar{\rho}^2\bar{T}^{-3\cdot5}L}{4\pi r^2} \tag{5}$$

---

* T. G. Cowling, *M.N.*, 94, 768, 1934.

outside the convective core. It is assumed here that the reader is familiar with the reason why a star must possess a convective core when the value of the index η in the energy generation formula is of order 15.* The symbols used in the above equations have the following meanings:—

r = distance from centre of star in cms.
$\mathfrak{R}$ = gas constant.
$\bar{\rho}$ = density in grams.
$\bar{T}$ = temperature in degrees A.
μ = mean molecular weight of stellar material.
G = constant of gravitation in c.g.s. units.
$\bar{M}(r)$ = mass contained in sphere of radius r in grams.
$L(r)$ = energy generated in sphere of radius r in ergs per sec.
E = constant in energy generation formula $\sim 1{\cdot}43 \cdot 10^{-126}$.
a = Stefan's constant in c.g.s. units.
c = velocity of light in cm. per sec.
α = coefficient of opacity $\sim 3.10^{+25}$.
X = fraction of hydrogen by mass per gram of stellar material.

It is of special interest to consider the case of a star satisfying the above equations, for in this case the solution is already known from outward computation. Accordingly this case provides a test of the proposed new method of computation, which if successful can then be applied to different problems that have not hitherto been investigated satisfactorily.

The parameter n defined by the following equation is of great value in the outward integration:—

$$n+1 = \frac{d(\log \bar{\rho}\bar{T})}{d(\log \bar{T})} \quad \begin{cases} = \gamma/(\gamma-1) & \text{inside the convective core} \\ = \dfrac{16\pi acG\mu}{3\mathfrak{R}\bar{\alpha}(1-X^2)L}\,\dfrac{\bar{M}\bar{T}^{6\cdot5}}{\bar{\rho}^2} & \text{outside} \quad ,, \quad ,, \end{cases} \tag{6}$$

for it is known that for $\bar{\rho}$ and $\bar{T}$ to tend to 0 together at the surface of the star the value of n must tend to 3·25 at the surface. This result can be seen by examining equations (1) and (5) near the surface, where $\bar{M}$, L may be regarded as constant. The numerical computation of equations (1), (2), (3) and (5) in the region outside the convective core must give a solution with n increasing outwards from $1/(\gamma-1)$ at the surface of the convective core to 3·25 at the surface of the star.

(*a*) *Procedure by Outward Integration.*—In practice auxiliary variables are defined to facilitate the computation, but the procedure can be described in terms of the variables given in the above equations. Let $\bar{\rho}(0)$, $\bar{T}(0)$ and $r = r_1$ be regarded as the variables in the problem, where $\bar{\rho}(0)$, $\bar{T}(0)$ are the central values of the density and temperature respectively and r_1 is the radius of the convective core. Inside the convective core the solution is given by Emden's equation for index $1/(\gamma-1)$, and for various values of γ these solutions have been tabulated. Suppose γ is given one of these special values, then the values of $\bar{\rho}(r)/\bar{\rho}(0)$, $\bar{T}(r)/\bar{T}(0)$, $d\bar{T}(r)/\bar{T}(0)dr$, $3\bar{M}/4\pi r^3\bar{\rho}(0)$ are known for $r < r_1$. At the surface of the convective core the value of $d\bar{T}/dr$ must be continuous, so that an equation is obtained giving a relation between the three variables r_1, $\bar{\rho}(0)$, $\bar{T}(0)$ by equating the value of $\dfrac{1}{\bar{T}(0)}\left(\dfrac{d\bar{T}(r)}{dr}\right)_{r=r_1}$ given by (5) with the value given by the Emden table. (Note that the value of $L(r_1)$ can clearly be computed in terms of r_1, $\bar{\rho}(0)$, $\bar{T}(0)$ from (3).) This leaves two variables, say r_1 and $\bar{\rho}(0)$. If specific values are given to r_1 and $\bar{\rho}(0)$, then equations (1), (2), (3) and (5) can be integrated outwards numerically. The value of r_1 is determined by the conditions that the parameter n must tend to 3·25 at the surface,

* *Cf.* for example *M.N.*, **102**, 180, 1942.

and the value of $\bar{\rho}(0)$ is determined by the requirement that $\bar{M}$ must tend at the surface to the assigned mass of the star. As explained in the introduction, these integrations are found to be extremely sensitive.

(*b*) *Procedure for Inward Integration.*—The procedure for inward integration will be described in detail by the introduction of suitable auxiliary variables. Let r_2 be a value of r such that $n(r_2)$ is very close to 3·25 (that is, $\bar{\rho} \propto \bar{T}^{3\cdot25}$ to good approximation for $r > r_2$) and define the dimensionless variable z by means of the equation

$$r = r_2 z. \tag{7}$$

Then except near the surface $z < 1$. Furthermore, define $\rho(z)$, $T(z)$, $M(z)$ by means of the relations

$$T(z) = \bar{T}(r)/\bar{T}(r_2), \qquad \rho(z) = \bar{\rho}(r)/\bar{\rho}(r_2), \qquad M(z) = \bar{M}(r)/\bar{M}(r_2), \tag{8}$$

so that $T = \rho = M = 1$ at $z = 1$. The equations (1), (2), (5) and (6) can be written in the form

$$\frac{d(\rho T)}{dz} = -\frac{\mu G \bar{M}(r_2)}{\mathfrak{R} r_2 \bar{T}(r_2)} \cdot \frac{\rho M}{z^2}, \tag{1'}$$

$$\frac{dM}{dz} = \frac{4\pi r_2^3 \bar{\rho}(r_2)}{\bar{M}(r_2)} \cdot \rho z^2, \tag{2'}$$

$$\frac{dT}{dz} = -\frac{3\bar{a}(1-X^2)L}{16\pi a c r_2} \cdot \frac{\left(\bar{\rho}(r_2)\right)^2}{\left(\bar{T}(r_2)\right)^{7\cdot5}} \cdot \frac{\rho^2}{T^{6\cdot5}} \cdot \frac{1}{z^2}, \tag{5'}$$

$$n+1 = \frac{16\pi a c G \mu}{3\mathfrak{R}\bar{a}L(1-X^2)} \cdot \frac{\bar{M}(r_2)\left(\bar{T}(r_2)\right)^{6\cdot5}}{\left(\bar{\rho}(r_2)\right)^2} \cdot \frac{MT^{6\cdot5}}{\rho^2}. \tag{6'}$$

Now by hypothesis $n(r_2) \sim 3\cdot25$, so that by putting $z = 1$ in (6′) we have

$$4\cdot25 = \frac{16\pi a c G \mu}{3\mathfrak{R}\bar{a}L(1-X^2)} \cdot \frac{\bar{M}(r_2)\left(\bar{T}(r_2)\right)^{6\cdot5}}{\left(\bar{\rho}(r_2)\right)^2}. \tag{9}$$

Write

$$\frac{3\bar{a}}{16\pi} \cdot \frac{(1-X^2)L}{a c r_2} \cdot \frac{\left(\bar{\rho}(r_2)\right)^2}{\left(\bar{T}(r_2)\right)^{7\cdot5}} = \Theta_2, \tag{10}$$

so that from (9)

$$4\cdot25\,\Theta_2 = \frac{G\mu\bar{M}(r_2)}{\mathfrak{R} r_2 \bar{T}(r_2)}. \tag{11}$$

The formulæ given above are all derived by rewriting the basic equations in terms of the newly defined quantities. If further we write

$$4\pi r_2^3 \bar{\rho}(r_2)/\bar{M}(r_2) = \Phi, \tag{12}$$

the equations to be solved are

$$\frac{d(\rho T)}{dz} = -4\cdot25\,\Theta_2 \frac{\rho M}{z^2}, \tag{13}$$

$$\frac{dM}{dz} = \Phi \rho z^2, \tag{14}$$

$$\frac{dT}{dz} = -\Theta_2 \frac{\rho^2}{T^{6\cdot5}} \cdot \frac{1}{z^2}, \tag{15}$$

subject to $\rho = T = M = 1$ at $z = 1$. If r_s is the radius of the star, then, since $\rho^2/T^{6\cdot5} = 1$ by hypothesis when $z \geqslant 1$, it follows from (7) and (15) that

$$r_2/r_s = (\Theta_2 - 1)/\Theta_2. \tag{16}$$

Accordingly the value of Θ_2 determines the relation of the distance r_2 to the radius of the star. It is shown below in section 3 that provided Θ_2 is not given such a value that r_2/r_s becomes too small for the approximation $\bar{\rho} \propto \bar{T}^{3\cdot25}$ to be applicable for $r_2 < r < r_s$, then the calculated value of the luminosity and radius of the star are independent of the particular value chosen for Θ_2. The position is therefore that the problem has been reduced to determining the parameters Φ, $\bar{\rho}(r_2)$, $\bar{T}(r_2)$ and r_2. The important point in the present method is that it is possible to determine Φ without first determining r_2, $\bar{\rho}(r_2)$ and $\bar{T}(r_2)$. Thus by working in terms of the ratios z, ρ, T, M the equations (13), (14), (15) have been written in a form that does not involve r_2, $\bar{\rho}(r_2)$ or $\bar{T}(r_2)$ explicitly. The conditions of fit of these equations on to the convective core are shown below to be sufficient to determine Φ. When Φ has been determined, equations (3), (9), (11) and (12) are sufficient to enable the numerical values of $\bar{\rho}(r_2)$, $\bar{T}(r_2)$, r_2 and L to be calculated. The problem of the calculation of L is considered in detail in the following section.

Let some particular numerical value be chosen for Θ_2 (the value should be $\geqslant 2$). Then the equations (13), (14), (15) contain only one parameter Φ, and the procedure to be followed is to assign trial values to Φ until a solution is obtained by the numerical integration of these equations for $z \leqslant 1$ that satisfies the following conditions. At some value of z, z_1 say, the numerical solution of (13), (14), (15) must fit on to the Emden solution of index $1/(\gamma - 1)$. The relevant value of z_1 to use for any given trial solution of (13), (14), (15) is evidently determined by the condition that the value of $(n+1)$ given by (6′) shall be equal to $\gamma/(\gamma - 1)$. Since $(n+1) = 4\cdot25$ when $z = 1$, this gives

$$4\cdot25 M(z_1)\big(T(z_1)\big)^{6\cdot5}/\big(\rho(z_1)\big)^2 = \gamma/(\gamma - 1), \tag{17}$$

where $M(z_1)$, $T(z_1)$, $\rho(z_1)$ are all known from the trial solution. The equation of fit to determine Φ is that the temperature gradient given by (15) must equal the temperature gradient given by the Emden solution at distance z_1 from the centre of the star. A difficulty arises, however, since the units of distance, temperature and density in (15) differ from the units in which the Emden solution is usually given. This can be seen from the following table:—

Units employed in (13), (14), (15)		*Units employed in Emden Solution*
Distance	$(\Theta_2 - 1)r_s/\Theta_2$	$\big[\mathfrak{R}\gamma\bar{T}(0)/4\pi(\gamma - 1)G\mu\bar{\rho}(0)\big]^{\frac{1}{2}}$
Density	$\bar{\rho}\big((\Theta_2 - 1)r_s/\Theta_2\big)$	$\bar{\rho}(0)$
Temperature	$\bar{T}\big((\Theta_2 - 1)r_s/\Theta_2\big)$	$\bar{T}(0)$

Thus if u is the radial co-ordinate in the Emden solution, then the value of u, u_1 say, corresponding to $z = z_1$, is evidently

$$\frac{r_s z_1 (\Theta_2 - 1)/\Theta_2}{[\mathfrak{R}\gamma\bar{T}(0)/4\pi(\gamma - 1)G\mu\bar{\rho}(0)]^{\frac{1}{2}}},$$

and using equations (11), (12) and (16) this can be written as:

$$\frac{u_1}{z_1} = \sqrt{\left\{\frac{4\cdot25(\gamma - 1)\Phi\Theta_2}{\gamma} \cdot \frac{\bar{\rho}(0)}{\bar{\rho}\big((\Theta_2 - 1)r_s/\Theta_2\big)} \cdot \frac{\bar{T}\big((\Theta_2 - 1)r_s/\Theta_2\big)}{\bar{T}(0)}\right\}}. \tag{18}$$

To solve this equation for u_1, the simplest procedure would appear to be a trial-and-error method. Thus, take a trial value for u_1, $u_1 = 1$ for example, then the Emden table gives

the numerical value of

$$\frac{\bar{\rho}(u_1)}{\bar{\rho}(0)}=\frac{\bar{\rho}\left((\Theta_2-1)\,.\,r_s/\Theta_2\right)}{\bar{\rho}(0)}\cdot\rho(z_1)=x \text{ say,}$$

so that

$$\frac{\bar{\rho}(0)}{\bar{\rho}\left((\Theta_2-1)\,.\,r_s/\Theta_2\right)}=\frac{\rho(z_1)}{x},$$

the value of x being known from the Emden table, and the value of $\rho(z_1)$ from the numerical solution of (13), (14) and (15). Similarly $y=\bar{T}(u_1)/\bar{T}(0)$ can be determined from the Emden table and $\bar{T}\left((\Theta_2-1)\,.\,r_s/\Theta_2\right)/\bar{T}(0)=y/T(z_1)$, and the value of u_1 can be computed immediately from (18). This calculated value gives a first approximation to the value of u_1, a second approximation being obtained by repeating this process. In this way a series of successive approximations is obtained for u_1; this series converges rapidly. The condition of fit the numerical computation must satisfy is that $(dT/dz)_{z=z_1}$ given by (15), when expressed in the same units as the Emden solution, must be equal to the temperature gradient given by the Emden solution. The value of $(dT/dz)_{z=z_1}$ given by (15), when expressed in the same units as the Emden solution, is

$$-\Theta_2\frac{\left(\rho(z_1)\right)^2}{\left(T(z_1)\right)^{6\cdot5}}\cdot\frac{1}{{z_1}^2}\cdot\frac{\bar{T}\left((\Theta_2-1)r_s/\Theta_2\right)}{\bar{T}(0)}\cdot\frac{z_1}{u_1}=-\left(\frac{\gamma\Theta_2 xy}{4\cdot25(\gamma-1)\Phi}\right)^{\frac{1}{2}}\cdot\frac{\left(\rho(z_1)\right)^{1\cdot5}}{\left(T(z_1)\right)^7}\frac{1}{{z_1}^2} \qquad (19)$$

which must be numerically equal to the temperature gradient given by the Emden table.

It will be seen that the use of the conditions of fit (17), (18), (19) will require a good deal of hand computation, but the amount of work involved in this procedure will be very much less than the work saved by the rapid numerical integration of (13), (14) and (15).

It may be noted that if the density, temperature and mass are expressed in c.g.s. units the conditions used in deriving (17), (18) and (19) require $\bar{\rho}(r)$, $\bar{T}(r)$, $d\bar{T}/dr$ and $d\log(\bar{\rho}\bar{T})/d\log\bar{T}$ to be continuous across the surface of the convective core. It follows immediately from the continuity of these quantities that $d\bar{\rho}/dr$ must also be continuous. Thus since both the Emden solution and the solution of (13), (14) and (15), when converted to c.g.s. units, satisfy equation (1) it follows that $\bar{M}(r)$ must be continuous. This means that $M(z_1)$ when expressed in the same units as the mass function in the Emden solution must be equal to the value of the Emden mass function at $u=u_1$.

3. *Calculation of the Luminosity.*—If the very small amount of energy generated outside the convective core is neglected, then it is easy to see from (3) that

$$L=4\pi E\left(\bar{\rho}(0)\right)^2\left(\bar{T}(0)\right)^{\eta}\{\Re\gamma\bar{T}(0)/4\pi(\gamma-1)G\mu\bar{\rho}(0)\}^{3/2}\int_0^{u_1}u^2\{\bar{T}(u)/\bar{T}(0)\}^{\eta+2/(\gamma-1)}du. \qquad (20)$$

The integral in (20) is given to good approximation by

$$\int_0^{u_s}u^2\{\bar{T}(u)/\bar{T}(0)\}^{\eta+2/(\gamma-1)}du,$$

where u_s is the largest value of u in the Emden solution and this integral can be computed directly from the Emden tables. On account of the large value of η the integral varies by only a small margin as γ varies from 5/3 to 4/3, and a value of 0·07 gives a good approximation whatever the value of γ in this range. Thus we may write

$$L=\left\{\frac{0\cdot28\pi E\left(\rho(z_1)\right)^{\frac{1}{2}}\left(T(z_1)\right)^{\eta+\frac{3}{2}}}{x^{\frac{1}{2}}y^{\eta+\frac{3}{2}}}\left[\frac{\Re\gamma}{4\pi(\gamma-1)G\mu}\right]^{\frac{3}{2}}\right\}\bar{\rho}^{\frac{1}{2}}(r_2)\bar{T}^{\eta+\frac{3}{2}}(r_2),$$

where the numerical value of the expression in the {} brackets is known once the required numerical solution of (13), (14) and (15) has been obtained. The factor

$\left(\bar{\rho}(r_2)\right)^{\frac{1}{2}}\left(\bar{T}(r_2)\right)^{\eta+\frac{3}{2}}$ may be eliminated from the expression for L by using (9), (11) and (12) to give

$$L=\left\{0{\cdot}28\pi\left[\frac{\gamma}{4\pi(\gamma-1)4{\cdot}25\Theta_2}\right]^{\frac{3}{2}}E\frac{\left(\rho(z_1)\right)^{\frac{1}{2}}\left(T(z_1)\right)^{\eta+\frac{3}{2}}}{x^{\frac{1}{2}}\,y^{\eta+\frac{3}{2}}}\right\}^{-\frac{1}{2\eta+5}}$$
$$\times\left(\frac{4\pi}{\Phi}\right)^{\frac{8\eta+25}{4\eta+10}}\left(\frac{G\mu}{4{\cdot}25\Theta_2\mathfrak{R}}\right)^{\frac{14\eta+45}{2\eta+5}}\left(\frac{16\Theta_2\pi ac}{3\bar{\alpha}(1-X^2)}\right)^{\frac{2\eta+6}{2\eta+5}}\bar{M}^{\frac{10\eta+31}{2\eta+5}},\qquad(21)$$

where $\bar{M}=\bar{M}\left((\Theta_2-1)r_s/\Theta_2\right)\sim\bar{M}(r_s)$ the mass of the star. It is seen that all quantities in (21) are known and the luminosity can therefore be calculated directly from this formula. Before discussing in detail the calculation of the luminosity, the result quoted above, that the value of L is independent of Θ_2, will be proved. The quantities Φ, $\rho(z_1)$, $T(z_1)$ depend on Θ_2 in a manner that can easily be determined, the remaining quantities in (21) apart from Θ_2 itself being independent of Θ_2. For r in the region in which $\bar{\rho}\propto\bar{T}^{3\cdot25}$ the value of $\bar{\rho}$ depends on r through the factor $\left((r_s/r)-1\right)^{3\cdot25}$. Thus if the value of Θ_2 is allowed to vary, the value of $\bar{\rho}\left((\Theta_2-1)r_s/\Theta_2\right)$ depends on Θ_2 through the factor $1/(\Theta_2-1)^{3\cdot25}$, whilst $\bar{T}\left((\Theta_2-1)r_s/\Theta_2\right)$ depends on Θ_2 through the factor $1/(\Theta_2-1)$.

Now from (12), (16)

$$\Phi=4\pi r_s^3\left(\frac{\Theta_2-1}{\Theta_2}\right)^3\bar{\rho}\left(\frac{\Theta_2-1}{\Theta_2}r_s\right)\Big/\bar{M}\left(\frac{\Theta_2-1}{\Theta_2}r_s\right),$$

so that since $\bar{M}\left((\Theta_2-1)r_s/\Theta_2\right)\sim\bar{M}(r_s)$ it is seen that

$$\Phi\propto\Theta_2^{-3}(\Theta_2-1)^{-0\cdot25},$$

whilst $\rho(z_1)$, $T(z_1)$ evidently depend on Θ_2 according to the proportionalities

$$\rho(z_1)\propto(\Theta_2-1)^{3\cdot25},\qquad T(z_1)\propto(\Theta_2-1).$$

It appears therefore that L depends on Θ_2 according to

$$\left[\Theta_2^{-\frac{3}{2}}(\Theta_2-1)^{\eta+\frac{6\cdot25}{2}}\right]^{-\frac{1}{2\eta+5}}\left[\Theta_2^3(\Theta_2-1)^{0\cdot25}\right]^{\frac{8\eta+25}{4\eta+10}}\Theta_2^{-\frac{14\eta+45}{2\eta+5}}\Theta_2^{\frac{2\eta+6}{2\eta+5}},$$

which is independent of Θ_2.

It remains to show that the present method leads to the same calculated values of the luminosity as the method of outward integration. This can be demonstrated since the numerical solution for the equations (13), (14) and (15) can be taken over from the solution already available for the case $\gamma=5/3$ from outward integration. The consistency of the present method with that given in a previous paper can then easily be established.* If u is measured in units of $[5\mathfrak{R}\bar{T}(0)/8\pi\mu G\bar{\rho}(0)]^{\frac{1}{2}}$, then the following table gives a selection of values from the solution given in a former paper,† this being a repetition of an integration given previously by Cowling.

	u	$\bar{\rho}(u)/\bar{\rho}(0)$	$\bar{T}(u)/\bar{T}(0)$	$\int^u dw\bar{\rho}(w)/\bar{\rho}(0)$
Surface of Convective Core	1·19			
	1·25	0·6722	0·7680	0·5165
	2·00	0·3305	0·5511	1·4668
	2·50	0·1712	0·4324	2·0736
	3·33	0·0471	0·2814	2·7314
	4·00	0·0148	0·1950	2·9775
	5·00	$1{\cdot}97.10^{-3}$	0·1045	3·1041
	6·97	0·00	0·00	3·1263

* F. Hoyle and R. A. Lyttleton, **102**, 177, 1942. † *Ibid.*, **102**, 219, 1942.

Choose Θ_2 so that $u=4z$, giving $z=1$ at $u=4$, and $z_s=1{\cdot}74$, from which it follows that $\Theta_2=2{\cdot}35$. Furthermore, from the values given in the above table for $u=4$ we have

$$\frac{\bar{\rho}\left((\Theta_2-1)r_s/\Theta_2\right)}{\bar{\rho}(0)}=\frac{x}{\rho(z_1)}=0{\cdot}0148,$$

$$\frac{\bar{T}\left((\Theta_2-1)r_s/\Theta_2\right)}{\bar{T}(0)}=\frac{y}{T(z_1)}=0{\cdot}1950.$$

The unit of u is evidently $r_2/4$, so that

$$\bar{M}(r_2)=4\pi\bar{\rho}(0)(r_2/4)^3\int_0^4 dw\, w^2\bar{\rho}(w)/\bar{\rho}(0),$$

which gives

$$\Phi=\frac{4\pi\bar{\rho}(r_2){r_2}^3}{\bar{M}(r_2)}=4^3\cdot\frac{\bar{\rho}\left((\Theta_2-1)r_s/\Theta_2\right)}{\bar{\rho}(0)}\cdot\frac{1}{\int_0^4 dw\, w^2\bar{\rho}(w)/\bar{\rho}(0)}$$

$$=\frac{4^3\times 0{\cdot}0148}{2{\cdot}9775}=0{\cdot}318.$$

All quantities appearing in (21) are therefore known and the luminosity can be calculated immediately. For the purposes of comparison with the previous paper consider the case $\bar{M}=5\odot$, $\mu=1$. Then putting

$$\eta=17{\cdot}25, \qquad E=1{\cdot}43.10^{-126}, \qquad \bar{\alpha}=3.10^{25},$$

the value of L given by (21) is $2{\cdot}3.10^{36}$ ergs per sec. in agreement with the luminosity calculated in the previous paper.

St John's College,
Cambridge:
1945 *January* 17.

METHOD OF OBTAINING AN ASTRO-FIX, USING A TABLE OF PREDETERMINED CALCULATIONS

J. H. Clarke

(Communicated by Professor W. M. Smart)

(Received 1944 March 9 *)

Summary

This paper presents a method of obtaining position lines at right angles and parallel to great circle routes. It will be found that a minimum amount of calculation is necessary during the actual flight.

Before the flight, calculate the altitude of a selected star as observed from the place of departure at the instant of its crossing the given great circle route. During the actual flight observe the star's altitude at a time as near as possible to the predetermined G.M.T. of its transit. The difference between these altitudes gives the distance run along the great circle route, from which a position line is obtained at right angles to the route.

Similarly, to obtain a position line parallel to the route, calculate before the flight the altitude of a suitable star when its azimuth is 90° different from the direction given by the great circle. During the actual flight observe this star's altitude as near as possible to this second predetermined time. Again the difference in altitudes enables a position line to be drawn.

If any observations are taken a minute or two before or after the proper G.M.T., a precomputed table enables a correction to be applied.

---

1. *Constants of the Great Circle between Two Positions.*—In order to test this method a great circle route passing through Wellington, N.Z., was calculated. Due to war-time restrictions on routes it was only possible to take the observations from the ground.

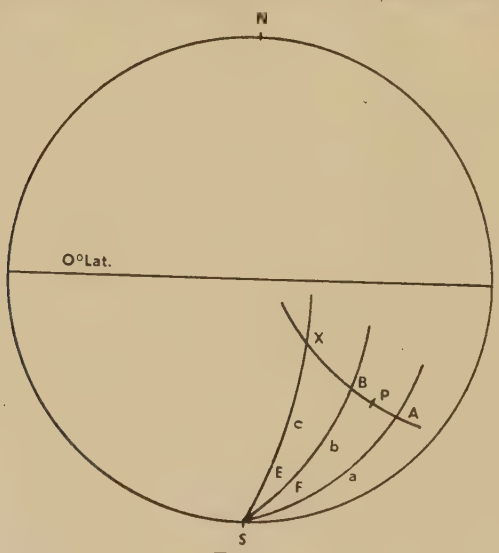

FIG. 1.

* Revised version received 1945 March 1.

A (56° 00′ S., 179° 00′ E.) Departure.
P (41° 13′ S., 174° 56′ E.) Wellington, N.Z.
B (36° 21′ S., 174° 00′ E.) Destination.
X Substellar point of star.
F Change of longitude A to B.
E L.H.A. of X with respect to meridian SB.

Determination of E.—By applying the four parts formula to triangles SAB, SBX in Fig. 1 and denoting SA, SB, SX by *a*, *b*, *c* respectively,

$$\cot a \sin b = \cot \hat{ABS} \sin F + \cos b \cos F$$

$$\cot c \sin b = \cot \hat{SBX} \sin E + \cos b \cos E.$$

Noting that $\cot \hat{ABS} = -\cot \hat{SBX}$ and eliminating these angles,

$$\cot b = \operatorname{cosec}(E+F)(\cot a \sin E + \cot c \sin F). \tag{1}$$

Expansion gives

$$\sin E(\cot b \cos F - \cot a) + \cos E(\cot b \sin F) = \cot c \sin F.$$

Divide throughout by the square root of the sum of the squares of the bracketed quantities, this divisor being denoted by *M*.

Then

$$M \sin(E+H) = \cot c \sin F, \tag{2}$$

where

$$\tan H = \frac{\sin F}{\cos F - \cot a \tan b} \tag{3}$$

and *M*, on simplification, is given by

$$M = \sqrt{(\cot^2 a + \cot^2 b - 2 \cot a \cot b \cos F)}. \tag{4}$$

Now let $\cot a = y$, $\cot b = z$.

By analogy with plane trigonometry we can draw the plane triangle, Fig. 2.

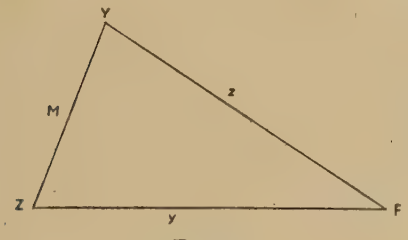

Fig. 2.

This is because

$$M^2 = y^2 + z^2 - 2yz \cos F.$$

Note that no approximation is being made.

Now the solution of the triangle FYZ is given by $\frac{1}{2}(Y+Z) = 90° - \frac{1}{2}F$, where *F* is known, and

$$\tan \tfrac{1}{2}(Y-Z) = \frac{y-z}{y+z} \cot \tfrac{1}{2}F.$$

Thus $\frac{1}{2}(Y-Z)$ is found and, since

$$\tfrac{1}{2}(Y+Z) + \tfrac{1}{2}(Y-Z) = Y, \tag{5}$$

we obtain *Y*. From the sine rule

$$M = \frac{y \sin F}{\sin Y} = \frac{\cot a \sin F}{\sin Y}.$$

Substituting for *M* in the expression (2), we have

$$\sin(E+H) = \frac{\cot c \sin Y}{\cot a}, \tag{6}$$

where *Y* is found by the method described in (5).

Since tan *H* is given by (3), the angle *E* may be determined.

The expression for the angle $(E+H)$ is ambiguous, but from practical considerations, no doubt arises as to the correct value of angle *E*.

There is only *one variable* for a constant route, namely c, the co-declination of the star chosen. This is of great assistance in preparing permanent tables for the route.

2. *Determination of the G.M.T. when a suitable Heavenly Body is directly over the Great Circle Route.*—Providing the great circle route does not run almost directly east and west, it is easy to select about two or three suitable navigational stars which will make their crossing of the route after sunset and before sunrise at a suitable altitude.

First calculate the L.H.A.'s of the 22 bright navigational stars with respect to the meridian of departure. The stars of course are then above the route. Actually there is no necessity to restrict the observations to the 22 brightest stars as several fainter stars, such as β Centauri, *Castor* and *Polaris*, are readily identified by navigators. Apart from small precessional changes each star will have a constant L.H.A., so that a list once prepared will be available for many years. The G.M.T. is found from the longitude of A and the *Air Almanac*.

Thus before a flight is undertaken it is a few minutes' work to decide from the list of L.H.A.'s which G.M.T.'s will be suitable for observation. This procedure is illustrated by an example in section 4.

3. *Obtaining the Position Line at Right Angles to the Route.*—First it is necessary to determine the altitudes of the navigational stars as seen from A at the instant of their crossing the great circle route, *i.e.* $90° - AX$, in Fig. 1. These constants may readily be determined by Dr. L. J. Comrie's method (see section 6).

As near as possible to the predetermined G.M.T., observe the altitude of the star. Should the time of observation differ by a minute or two from the precomputed G.M.T. apply a simple correction from a table, which is again constant for the route. (See section 5.)

The difference between the observed and calculated altitudes gives the distance run along the great circle which is then marked by a point. In normal times an aircraft or vessel approximates closely to the great circle by a series of rhumb lines. Then a short line perpendicular to the route through this point gives the position line appropriate to the G.M.T. of observation.

This process can naturally be repeated for the other stars available for observation during the flight.

The basic idea of obtaining the distance run along a great circle is, I believe, due to Squadron Leader P. E. Hudson, R.N.Z.A.F., but the foregoing method eliminates solving a series of spherical triangles and provides constants for the route. In addition the errors introduced by observing at times a few minutes different from those computed are investigated (see section 5).

4. *Example.*—The Sun was used for convenience of observation. On 1943 November 17 at $01^h\ 00^m$ G.M.T. the declination of the Sun was 18° 44′ S., hence $c = 71° 16'$. Then using the positions A, P, B in section 1, as shown in Fig. 1,

$$Y = 170° 07\tfrac{1}{2}' \quad \text{and} \quad E = 2° 38\tfrac{1}{2}'.$$

The L.H.A. with respect to the departure meridian SA is therefore $7° 38\tfrac{1}{2}'$. From the *Air Almanac* it is found that at $00^h\ 19^m\ 25^s$ G.M.T. the Sun has this value for L.H.A. Also the altitude as observed from A is found by calculation to be $52° 17\tfrac{1}{2}'$.

By a theodolite observation the altitude of the Sun (corrected for refraction) was found to be 67° 19′ at Wellington, position P (Fig. 1), at $00^h\ 19^m\ 30^s$, 1943 November 17.

It may safely be assumed that a difference of 5 seconds will not introduce a noticeable error in navigation. The difference in altitudes, *i.e.* $15° 01\tfrac{1}{2}'$, gives the distance AP (Fig. 1).

Calculation gives the actual great circle distance AP, assuming from section 1 the exact position of P, as 15° 01′—a very close agreement.

5. *Correction for Error in Time of Observation.*—The following is an extension of

the principles discussed in the *Admiralty Manual of Navigation*, Vol. III, 1938, Chapter XII.

(*a*) *First regard the Observer as Stationary.*—If t = error in seconds of time, then $t/4$ = error in L.H.A. expressed in minutes of arc. Also if δh = change in altitude in minutes of arc,

$$\delta h = \tfrac{1}{4}t \cos (\text{lat.}) . \sin (\text{azimuth}), \qquad (7)$$

It will be sufficiently accurate here to use the mean latitude between A and B and take the azimuth from the chart.

Now as the star is to the west of the observer when on or near the great circle route AB, its altitude is decreasing after the predetermined G.M.T.

(*b*) *Allowance for moving Observer.*—Let the track or course made good be represented by C, and the average speed be S nautical miles per minute.

$$\text{The north component} = S \cos C. \qquad (8)$$
$$\text{The west component} = -S \sin C. \qquad (9)$$

The term (8) has the effect of bringing the star nearer to the observer who may now be considered at rest.

In Fig 3,

X = former substellar point.
X′ = new substellar point.
P = position of observer.

If PQ is made equal to PX′ then XX′Q may be regarded as a plane right-angled triangle.

XX′ = δd = change in declination obtained from (8).
XQ = $\delta h'$ = change in altitude.

Thus

$$\delta h' = \delta d \cos \text{SXP}. \qquad (10)$$

The angle SXP may be obtained sufficiently accurately by a chart measurement or by the use of a Navicard.* The altitude increases in this case for a late observation.

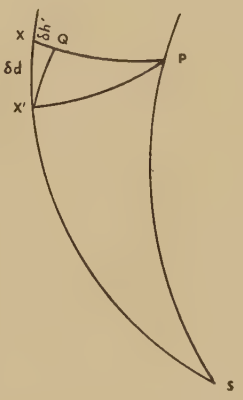

Fig. 3.

The term (9) has the effect of reducing the L.H.A. West. Now in deriving (7) the L.H.A. was assumed to be changing by 15′ per minute of time. Thus using (9) we correct (7) by multiplying it by $(15 + S \sin C)/15$.

Hence the complete correction for a moving observer is

$$\left(\frac{15 + S \sin C}{15}\right)\delta h + \delta h', \qquad (11)$$

where δh and $\delta h'$ are given by (7) and (10).

Thus a set of tables may be drawn up for the route which will be constant for each star.

(*c*) *Example.*—On the same day at $00^h\ 23^m\ 17^s$ the Sun's altitude was 67° 10′ (corrected for refraction). Substituting $t = 232$ sec., mean lat. 46° S., azimuth 351° in (7) gives the corrected *observed* altitude as 67° 16½′ at $00^h\ 19^m\ 25^s$, which is in good agreement with the altitude 67° 19′ (section 4).

It has not been possible as yet to obtain actual figures for a moving observer, so the following is supplied merely as an illustration.

Airspeed, which may be taken here as approximately equal to the ground speed, = 150 knots and the angle SXP = 7° (see Figs. 1 and 3).

* See Professor F. Debenham's *Astrographics*.

Substituting in (11) the correction to apply for an observation 100 sec. late, is $(2{\cdot}7-4{\cdot}1)'$.

Thus had the altitude been 67° 22′ at $00^h\ 21^m\ 05^s$ G.M.T., the altitude at the predetermined time would have been 67° 20½′.

6. *Obtaining a Position Line Parallel to the Great Circle Route.*

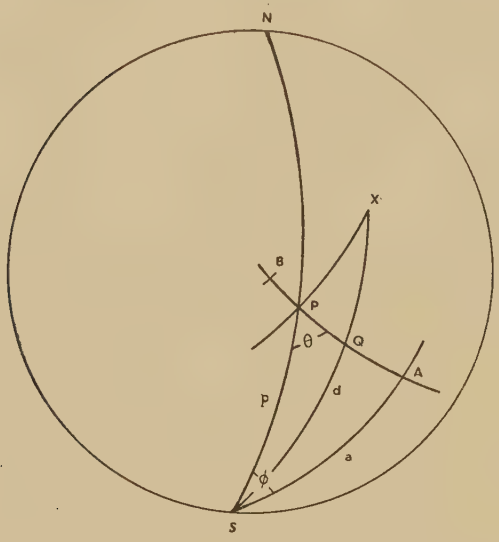

FIG. 4.

(*a*) Select suitable spaced points $P_1, P_2, \ldots$, *e.g.* at 120′ intervals, along the route.

(*b*) By referring to a globe or by the use of a Navicard (see section 5 (*b*)) determine suitable stars with azimuths approximately perpendicular to the route at some time on their circle of declination. Eliminate stars low in the sky.

(*c*) Calculate exactly by the method given below in (*h*) the constant L.H.A.'s, relative to P_1, P_2 ..., of these selected stars and the altitudes as seen from P_1, P_2, ...

(*d*) Prior to the actual flight determine the most suitable points and corresponding stars, being guided by consideration of altitudes as seen from P_1, P_2, ...

(*e*) During the actual flight decide which of the points P_1, P_2, . . . will be suitable for observation. Section 4 naturally aids in the determination of the position of the aircraft.

(*f*) As near as possible to the predetermined time at which the star's azimuth differs by 90° from the bearing of the great circle route observe the actual altitude of the star.

(*g*) The position line is then drawn on the chart parallel to the route towards or away from the star according as the observed altitude is greater or less than the calculated altitude.

(*h*) *Calculation of L.H.A. of a Selected Star X for the Position P.*—P is a known position on the route marked on the chart (Fig. 4). From the triangle ASP the angle $APS = \theta$ is easily determined since a, p, and the change of longitude $ASP = \phi$, are known. It is an advantage here to use Dr. L. J. Comrie's short-cut method using Hughes's *Sea and Air Navigation Tables*. Other short-cut methods are only applicable if ϕ is an integral number of degrees.*

In Fig. 4 let the great circle PX which is at 90° to the route AB cut the star's declination circle at X. Draw the great circle SX cutting AB at Q. Denote SP by p and SX by d. Then in the triangle PSX we know p (the co-latitude of P) and d (the co-declination) and the angle $SPX = 90° + \theta$.

Hence the angle SXP is determined by the sine rule, and Napier's analogies, which are suitable for use with logarithms, enable PSX, the LHA, and PX to be found.

7. *Example.*—Using the same route as before the star Rigel was observed on 1943 November 17. This corresponds to P at Wellington, where again ground observations were taken.

* See *Admiralty Navigation Manual*, Vol. III, p. 114, 1938.

When the relative bearing of Rigel is exactly 90° from the route, $\theta = 8° 45\frac{1}{2}'$. Angle SXP has the only possible solution of 48° 42′. Finally Napier's analogies gives the L.H.A. of Rigel = 67° 31′ and the calculated altitude at that time = 22° 18′.

Corresponding to the longitude of P (174° 56′ E.) and Rigel, the G.H.A. Aries is 195° 30′.

The *Air Almanac* shows that G.H.A. Aries has this value at $09^h\ 19^m\ 47^s$ G.M.T.

Observation 5 sec. earlier than the computed time gave 22° 19′ as the observed altitude of Rigel (corrected for refraction); this value is in satisfactory agreement with the value just calculated.

Had the altitude at that time been 22° 30′, then a position line 12′ on the star's side of the route would have been drawn parallel to the great circle route near Wellington. Fig. 5 shows a few of the stars available for finding both types of position lines when flying on the route discussed.

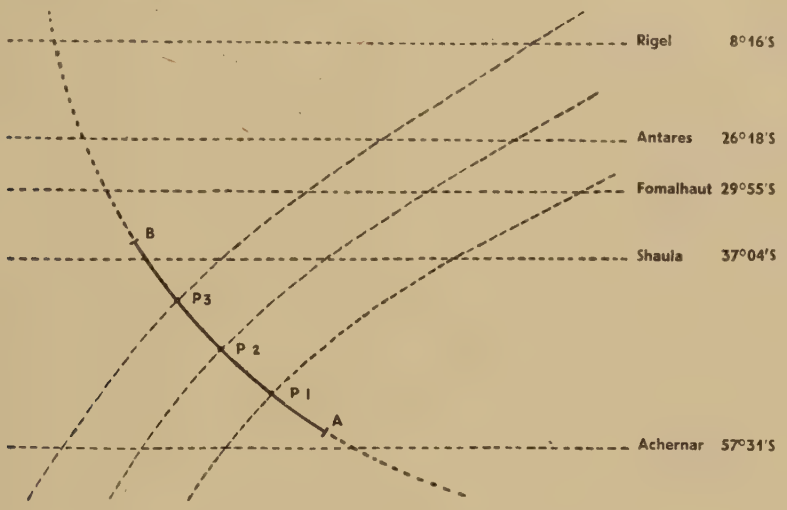

FIG. 5.

8. *Correction to be applied for Error in Time when Drawing Position Lines Parallel to the Route.*—A paper by W. M. Smart * shows that the position line will not be altered substantially if the observations are made for any position of the observer within a degree or so of the point P for which the calculations are made.

If an error in time is made, the corrections to be applied may be discussed as in section 5, due regard being paid to the angles involved. However, for this type of position line it is perhaps an over-refinement.

9. *Conclusion.*—It will be noted that it is not necessary to perform trigonometric calculations or even refer to an *Air Almanac* during a flight if this method is used.

The paper may suggest simplifications and other alternatives to those engaged in shortening the work of navigation.

The writer is especially indebted to Professor W. M. Smart for suggestions regarding the presentation of this paper.

Seddon Memorial Technical College,
Auckland, N.Z.

* *M.N.*, 79, 520, 1919.

THE ORBIT OF I 260, β_2 TUCANÆ ($0^h\ 27^m.0$, $-63°\ 31'$)

W. P. Hirst

(Communicated by W. H. van den Bos)

(Received 1945 March 9)

A preliminary orbit of this rather difficult pair was published by van den Bos in 1927.* It was based on a series of measures, mainly by Innes, prior to 1917 together with van den Bos's own measures in 1925 and 1926. The pair has made more than a complete revolution since its discovery, and at Dr. van den Bos's suggestion an attempt has been made to get a rather more accurate orbit. The task was made difficult by the fact that actual measures extend over only 100°, while the earlier distances are clearly unreliable. To complicate matters further, there is a systematic discrepancy between the measures made by van den Bos on the one hand and Voûte on the other in the most critical part of the arc—that following periastron from 1925 to the early 1930's. The measures of both observers are internally consistent, but they indicate two quite distinct arcs which join up about 1932. This refers to the angles; the distances, unfortunately, have too wide a spread to give much guidance.

For two reasons the greater weight was given to van den Bos's figures: firstly, because the pair was low for Voûte; and secondly, because the Johannesburg measures agree better with the distances, such as they are.

The following elements were obtained by solving a roughly drawn apparent ellipse by Zwiers's method and then correcting differentially by rough graphical methods, using the angle residuals only. The semi-axis major rests on the wider distances by the modern instruments:—

					″
P	43·07 years	i	131°·2	A	−0·1567
T	1920·66	ω	293°·8	B	+0·2527
e	0·770	Ω	65°·6	F	+0·2542
n	8°·359	a	0″·411	G	+0·2966

The ephemeris for one revolution is:—

Epoch	θ	ρ	Epoch	θ	ρ
	°	″		°	″
1947·81	290·3	0·54	1963·92	100·0	0·08
52·87	279·5	0·50	65·09	49·7	0·16
56·95	268·5	0·44	65·87	34·6	0·19
58·99	260·6	0·36	67·03	18·9	0·23
59·99	255·5	0·31	68·95	1·0	0·28
61·01	248·1	0·26	71·01	347·4	0·32
62·05	235·4	0·18	73·00	337·4	0·36
62·89	211·0	0·11	75·99	325·8	0·42
63·25	184·9	0·08	78·66	317·7	0·46
63·62	138·0	0·06	84·71	303·0	0·52

The residuals are shown in the following table. There is still room for considerable improvement, but the available material hardly warrants further correction at present. After the next periastron a more reliable orbit should be obtainable.

* *B.A.N.*, 3, 260, 1927.

Measures of I 260

Date	θ_0	O − C or (θ_c)	ρ_0	O − C or (ρ_c)	Nights	Aperture	Observer
	°	°	″	″		Inch	
1896·0	335 est.	+ 26·2	0·4	−0·10	1	13	Bailey
1897·9	300 est.	− 4·4	0·7	+0·18	1	7	I.
1900·36	297·9	− 1·3	0·76	+0·23	2, 1	18	I.
0·71	302·9	+ 4·4	0·81	+0·28	1	18	Lunt
1·58	293·1	− 3·6	0·94	+0·40	3, 2	18	I.
9·8	300 est.	+ 20·5	0·4	−0·10	1	9	I.
11·00	240? est.*	− 36·6		(0·49)	1	9	I.
11·00	290 est.	+ 13·4	0·6	+0·11	1	9	I.
11·04	276·7	+ 0·2	0·34	−0·16	4, 3	9	I.
11·93	272·3	− 1·9	0·66	+0·19	2	9	I.
12·93	270·2	− 1·2	0·74	+0·29	3	9	I.
13·88	268·7	+ 0·2	0·67	+0·23	4	9	I.
14·91	265·5	+ 0·7	0·65 †	+0·26	4	9	I.
15·92	260·9	+ 0·3	0·67 †	+0·31	4, 2	9	I.
16·81	268·0	+ 11·9	0·37	+0·05	1	17	δ.
16·82	too close	(256·0)		(0·32)	1	17	δ.
16·92	255·2	− 0·3	0·47	+0·16	2	9	I.
17·94	257?	+ 8·9		(0·26)	1	9	I.
20·85	too close	(100·0)		(0·08)	3	17	δ.
22·02	round	(49·7)		(0·16)	1	17	δ.
22·80	too close	(34·6)		(0·19)	1	17	δ.
23·96	round	(18·9)		(0·23)	1	17	δ.
25·88	1·7	+ 0·7	0·17	−0·11	6	26	B.
26·84	354·0	− 0·1	0·24	−0·06	7	26	B.
27·94	348·0	+ 0·6	0·24	−0·08	5	26	B.
28·85	342·5	0·0	0·33	−0·01	4	26	B.
29·58	344·6	+ 5·6	0·42	+0·06	6	24	V.
29·93	336·8	− 0·6	0·30	−0·06	3	26	B.
30·54	338·4	+ 3·6	0·44	+0·06	4	24	V.
30·74	336·4	+ 2·5	0·36	−0·02	4	26	B.
31·84	330·0	+ 0·3	0·36	−0·04	4	26	B.
32·56	332·0	+ 4·9	0·43	+0·02	3	24	V.
32·81	322·0	− 4·2	0·50	+0·08	1	17	δ.
32·92	325·5	− 0·3	0·41	−0·01	6	26	B.
33·52	325·2	+ 1·3	0·44	+0·01	4	24	V.
33·86	322·9	+ 0·1	0·47	+0·04	4	26	B.
34·58	320·2	− 0·4	0·55	+0·11	4	24	V.
34·85	319·4	− 0·4	0·47	+0·02	2	26	B.
35·59	318·2	+ 0·5	0·61	+0·15	5	24	V.
35·85	312·6	− 4·3	0·56	+0·10	1	17	δ.
36·91	313·9	− 0·2	0·44	−0·04	1	26	φ.
37·56	311·8	− 0·6	0·55	+0·07	4	24	V.
37·85	312·7	+ 1·0	0·50	+0·01	4	26	B.
38·79	308·0	− 1·5	0·54	+0·04	4	26	B.
41·64	301·1	− 1·9	0·5 est.	−0·02	1	7	Hirst
41·79	301·4	− 1·3	0·51	−0·01	4	26	B.
43·10	294·1	− 5·8	0·4 est.	−0·13	1	7	Hirst
43·80	293·0	− 5·4	0·43 est.	−0·10	2	7	Hirst
44·75	297·5	+ 1·0	0·45 est.	−0·09	1	7	Hirst
44·95	296·6	+ 0·5	0·56	+0·02	2	26	B.

* Noted "Doubtful". † Noted "Too large".

Cape Town:
1945 *January* 25.

THE ORBIT OF I 65, $6^h\ 53^m{\cdot}7$, $-35°\ 22'$ (1900)

W. P. Hirst

(Communicated by W. H. van den Bos)

(Received 1945 March 9)

This pair was discovered by Innes with the Cape 7-inch when the distance was $0''{\cdot}26$—a remarkable performance. He followed up his discovery with a fine series of measures, first with the Maclean 18-inch at the Cape and later with the Johannesburg 9-inch.

Using these and a few measures by Voûte, van den Bos and himself after the 1925 periastron, Finsen computed an orbit (*U.O. Circ.*, 86, 1932).

					″
P	16·5 years	i	56°·3	A	+0·157
T	1926·8	ω	269°·7	B	+0·076
e	0·586	Ω	116°·4	F	−0·139
n	21°·818	a	$0''{\cdot}315$	G	+0·282

The next observed periastron was passed in 1942, and in view of the fact that we now have a complete revolution covered by the modern instruments (Johannesburg $26\frac{1}{2}$-inch and Lembang 24-inch) it seemed worth while to re-compute in an effort to get a more definite orbit.

An attempt to correct Finsen's elements differentially showed them to be too much in error for direct differential correction; a fresh orbit was accordingly computed from the measures from 1928 and this was then corrected differentially from all the measured angles, using the method previously published.* The semi-axis major was obtained by comparison with the distances measured from 1930 to 1936. The following elements were obtained:—

					″
P	16·70 years	i	37°·2	A	+0·1950
T	1925·54	ω	224°·1	B	+0·0190
e	0·3832	Ω	147°·9	F	−0·0617
n	21°·557	a	$0''{\cdot}216$	G	+0·1845

The ephemeris for one revolution is:—

	θ	ρ		θ	ρ
	°	″		°	″
1945·80	135·2	0·22	1954·90	245·3	0·19
46·88	148·9	0·26	55·85	265·9	0·18
47·94	160·1	0·27	56·91	292·8	0·16
48·88	169·1	0·28	57·88	321·9	0·15
49·88	178·6	0·28	58·82	359·6	0·12
50·87	188·4	0·27	59·50	36·6	0·11
51·86	199·2	0·25	59·91	60·3	0·12
52·79	210·7	0·24	60·85	100·4	0·15
53·80	225·6	0·21	61·51	117·7	0·18

The measures and residuals are given in the table below:—

* *M.N.*, 103, 337, 1943.

Measures of I 65

Date	θ_0	O − C or (θ_c)	ρ_0	O − C or (ρ_c)	n	Aperture Ins.	Obs.	Remarks
	°	°	″	″				
1896·6	150 est.	− 0·3	0·6 est.	+0·34	1	7	I.	
97·3	160 est.	+ 5·5		(0·27)	1	7	I.	
98·3	190·3	+ 25·8	0·26	−0·02	1	24	See	
1900·01	184?	+ 3·2		(0·28)	1	18	I.	Perhaps elongated.
0·06	184·9	+ 3·6	0·3 est.	+0·02	1	18	I.	In contact.
0·98	192·6	+ 2·0	0·25 est.	−0·02	1	18	I.	Elongated.
1·13	191·8	− 0·4	(0·46)	(0·26)	1	18	I.	Slightly elongated.
1·97	208·3	+ 6·6	(0·72)	(0·25)	1	18	I.	Slightly elongated.
2·30	207·6	+ 1·9		(0·24)	1	18	I.	Not too sure.
3·18	216·3	− 1·3	0·30	+0·07	3	18	I.	
8·3	300 est.	− 41·2		(0·14)	1	9	I.	
11·05		(109·0)		(0·17)	1	9	I.	Not single.
12·30	135 * est.	+ 1·4		(0·22)	1	9	I.	Doubtful.
13·18	143·8 *	− 1·7	0·3 est.	+0·05	1	9	I.	Very slightly oval.
14·07	150 est.	− 5·3		(0·27)	1	9	I.	Doubtful.
16·10	175 *·0	0·0	0·4 est.	+0·12	1	9	I.	Very slightly oval.
16·29	190 est.	+ 13·2		(0·28)	1	9	I.	Practically round.
1917·10	178 * est.	− 6·7		(0·27)	1	9	I.	Poor.
20·09	227·2	+ 6·5	0·32	+0·10	2	17	δ.	
26·10	94·2 *	+ 57·6	0·18 est.	+0·07	1	26½	B.	Doubtful.
26·22		(43·7)		(0·11)	2	26½	B.	Single.
28·11	118·1	+ 0·4	0·21	+0·03	5	26½	B.	
29·10	133·7	− 1·5	0·28	+0·06	4	26½	B.	
29·80	146·2	+ 1·7	0·28	+0·03	5	24	V.	
30·18	146·6	− 2·3	0·26	0·00	4	26½	φ.	
30·20	147·6	− 1·6	0·28	+0·02	6	26½	B.	
30·87	155·8	− 0·5	0·27	0·00	4	24	V.	
31·09	158·3	− 0·2	0·28	+0·01	4	26½	φ.	
31·24	160·4	+ 0·3	0·28	+0·01	5	26½	B.	
32·04	167·5	− 0·3	0·27	−0·01	6	26½	B.	
32·18	169·9	+ 0·8	0·28	0·00	4	26½	φ.	
32·80	175·7	+ 0·7	0·28	0·00	4	24	V.	
33·11	178·3	+ 0·4	0·27	−0·01	6	26½	B.	
33·18	179·8	+ 1·2	0·26	−0·02	4	26½	φ.	
33·84	183·4	− 1·6	0·27	0·00	4	24	V.	
34·09	188·7	+ 1·1	0·27	0·00	4	26½	B.	
34·16	193·0	+ 4·7	0·23	−0·04	2	17	δ.	
34·16	194	+ 5·7	0·240	−0·030	2	26½	φ.	Interferometer.
34·17	195	+ 6·6	0·278	+0·010	4	26½	B.	Interferometer.
34·17	192·0	+ 3·6	0·26	−0·01	5	26½	φ.	
34·83	194·2	− 1·3	0·25	−0·01	4	24	V.	
35·06	197·8	− 0·2	0·24	−0·01	6	26½	B.	
35·16	198·3	− 0·9	0·25	0·00	3	17	δ.	
35·82	205·2	− 2·0	0·26	+0·02	5	24	V.	
35·85	207·9	+ 0·3	0·25	+0·01	2	24	B.	(At Lembang.)
36·09	210·9	+ 0·2	0·25	+0·01	6	26½	B.	
36·86	221·9	+ 0·2	0·22	0·00	4	24	V.	
37·10	222·9	− 2·7	0·24	+0·03	6	26½	B.	
37·84	243·3	+ 4·9	0·22	+0·02	4	24	V.	
38·20	249·9	+ 4·6	0·21	+0·02	4	26½	B.	
38·86	255·2	− 4·0	0·22	+0·04	4	24	V.	
39·15	265·3	− 0·6	0·19	+0·01	4	26½	B.	
40·21	287·7	− 5·1	0·20	+0·04	2	26½	B.	
41·18	328·7	+ 6·8	0·18	+0·03	3	26½	B.	
42·12	339·3	− 20·3	0·16	+0·04	1	26½	B.	
44·15	102·5	+ 2·1	0·17	+0·02	5	26½	B.	

Note.—Angles marked * have been decreased by 180°.

Cape Town:
1945 *January* 27.

V 380 SCORPII

F. M. Bateson

(Received 1945 February 28)

Summary

Further observations are here published, making some 381 estimates available for discussion. Elements have been deduced from these, and it is suggested that V 380 Scorpii belongs to the semi-regular type of variables.

---

1. Variability of 10·6 to 11·3 photographic was discovered in the star CoD – 30° 13620 by Miss A. J. Cannon in 1925.* It was rediscovered by F. M. Bateson, who published visual observations of the Variable Star Section of the N.Z. Astronomical Society.† Position for 1900 is R.A. $16^h\ 49^m\ 46^s$, Dec. S. 30° 09′·2; Spectrum, Ma; Designation, V 380 Scorpii.

2. Observations have been continued from New Zealand by the following observers:—

Name	Place	Instrument	Abbr.
Bateson, F. M.	Whangarei	3½-inch refractor	Bt.
Drew, W. A. H.	Dunedin	3-inch ,,	Dr.
Hobbs, W. H.	Dunedin	3-inch ,,	Ho.
Jones, A.	Timaru	5-inch reflector	Jo.
Smith, G. S.	Dunedin	2·45-inch refractor; 6½-inch reflector	Sm.

The present note is based on the estimates now published and those previously printed.† All estimates were made by the Fractional Method, using the Harvard sequence. Table I gives the J.D. of observation, the magnitude derived from the estimate and the observer's abbreviation.

Comparison stars were ‡:—

CoD	R.A. 1900	Dec. 1900	Mag.
	h m s	° ′	
– 30° 13581	16 47 44	S. 30 35·7	8·68
13652	16 51 55	30 17·4	9·86
13612	16 49 15	30 29·4	10·23
13622	16 50 04	30 05·8	10·62
13634	16 50 46	30 11·1	10·84

On account of the position of V 380 Scorpii it is not observable from New Zealand for four months each year. Due also to the war services of the observers the observations over the past five years have lacked the continuity of previous years.

3. Table II lists the observed dates of maxima and minima. The columns give for maxima and minima respectively: Observed J.D., magnitude, weight on scale of 1 (poor) to 5 (good, curve considered complete and reliable), interval from the immediate preceding maximum or minimum, when such has been observed, and the difference O – C as derived from the period given below.

* *Harvard Bulletin*, No. 825, 1925.
† *A.N.*, Nr. 6190, 1936.
‡ *Harvard Annals*, 63, part 2, 1913.

TABLE I

Observations of V 380 Scorpii

J.D. 242....	Mag.	Obs.	J.D.	Mag.	Obs.	J.D. 243....	Mag.	Obs.
8249·0	9·5	Sm.	2428750·0	10·3	Sm.	1250·8	9·9	Jo.
8251·9	10·2	Sm.	8804·9	10·3	Sm.	1251·8	9·9	Jo.
8254·0	9·5	Sm.	8815·9	10·2	Sm.	1252·9	9·9	Jo.
8256·9	9·5	Sm.	8839·9	10·4	Sm.	1253·8	10·0	Jo.
8273·0	9·8	Bt.	8841·9	10·4	Sm.	1254·8	10·1	Jo.
8274·0	9·9	Sm.	8980·0	9·5	Sm.	1255·8	10·1	Jo.
8275·0	10·4	Bt.	8982·0	9·5	Sm.	1257·8	10·0	Jo.
8275·9	10·2	Dr.	8991·9	9·5	Sm.	1258·8	10·1	Jo.
8275·9	9·9	Sm.	8996·9	9·5	Sm.	1259·8	9·9	Jo.
8276·0	9·8	Bt.	8997·9	9·5	Sm.	1260·8	10·2	Jo.
8284·9	10·0	Dr.	9010·9	9·5	Sm.	1261·8	10·1	Jo.
8285·0	10·0	Sm.	9019·9	9·5	Sm.	1264·8	10·1	Jo.
8292·0	10·0	Sm.	9021·9	9·5	Sm.	1265·8	10·1	Jo.
8297·9	9·5	Sm.	9023·8	9·5	Sm.	1269·0	10·1	Jo.
8301·0	9·4	Sm.	9026·9	9·7	Sm.	1271·8	10·1	Jo.
8302·0	9·4	Sm.	9040·9	9·5	Sm.	1273·2	9·9	Jo.
8308·0	9·7	Sm.	9101·9	10·0	Sm.	1279·8	10·2	Jo.
8308·9	9·5	Sm.	9163·9	10·0	Sm.	1282·8	10·2	Jo.
8309·9	9·5	Sm.	9472·8	10·2	Sm.	1284·8	10·0	Jo.
8310·8	9·5	Sm.	9481·9	10·0	Sm.	1290·8	9·9	Jo.
8311·9	9·6	Bt.	9543·8	10·4	Sm.	1292·9	10·2	Jo.
8319·0	10·2	Sm.	9545·9	10·4	Sm.	1294·9	10·1	Jo.
8321·0	9·9	Sm.	9716·9	10·2	Sm.	1295·9	10·2	Jo.
8332·0	10·0	Sm.	9721·9	10·4	Sm.	1309·8	10·1	Jo.
8334·0	10·1	Sm.	9734·9	10·4	Sm.	1312·9	9·9	Jo.
8336·0	10·2	Sm.	9741·0	10·2	Sm.	1314·0	10·1	Jo.
8337·0	10·2	Sm.	9749·0	9·6	Bt.	1314·9	10·2	Jo.
8338·9	10·0	Bt.	9751·9	9·9	Sm.	1315·8	10·2	Jo.
8339·8	10·0	Bt.	9751·9	9·8	Bt.	1316·8	10·1	Jo.
8340·9	10·4	Sm.	9779·9	9·9	Sm.	1320·8	10·2	Jo.
8341·8	10·2	Bt.	9785·9	10·1	Sm.	1324·8	10·0	Jo.
8341·8	10·0	Sm.	9791·9	9·9	Sm.	1327·9	9·9	Jo.
8342·8	9·8	Bt.	9801·9	9·9	Sm.	1337·8	10·0	Jo.
8343·9	10·0	Sm.	9803·9	9·9	Sm.	1338·9	9·9	Jo.
8343·9	9·8	Bt.	9809·9	9·9	Bt.	1339·9	9·7	Jo.
8357·8	10·4	Bt.	9811·8	9·5	Sm:	1342·8	9·7	Jo.
8359·9	10·4	Sm.	9856·9	9·9	Ho.	1344·8	9·7	Jo.
8364·9	10·2	Sm.	9856·9	9·9	Sm.	1345·8	9·9	Jo.
8365·8	10·4	Sm.	9862·9	10·2	Sm.	1346·8	10·0	Jo.
8369·9	10·4	Sm.	9865·9	9·9	Sm.	1349·8	9·9	Jo.
8371·8	10·5	Sm.	9866·0	9·9	Bt.	1353·0	9·6	Jo.
8393·0	10·4	Sm.	9866·9	10·1	Sm.	1353·9	9·9	Jo.
8393·9	10·3	Sm.	9872·9	10·7	Ho.	1353·9	10·2	Bt.
8394·9	10·2	Sm.	9872·9	10·1	Sm.	1369·9	9·7	Jo.
8397·9	10·4	Sm.	9875·9	9·6	Bt.	1371·9	9·7	Jo.
8425·9	10·2	Sm.	9877·9	9·9	Bt.	1372·9	10·0	Bt.
8428·9	10·2	Sm.	9880·9	10·2	Sm.	1373·8	10·0	Bt.
8430·9	10·0	Sm.	9884·0	9·9	Sm.	1373·9	9·7	Jo.
8431·9	9·7	Sm.	9884·8	10·5	Sm.	1374·9	9·7	Jo.
8450·9	10·1	Sm.	9899·9	10·3	Bt.	1376·9	9·6	Jo.
8640·9	9·5	Sm.	2429913·9	10·5	Sm.	1378·9	9·9	Jo.
8643·9	9·5	Sm.	2430119·9	9·7	Sm.	1379·8	10·5	Bt.
8695·9	9·5	Sm.	0135·9	9·9	Bt.	1380·9	10·3	Bt.
8715·9	10·4	Sm.	0139·9	10·0	Bt.	1380·9	9·6	Jo.
8716·8	10·4	Sm.	0218·8	10·0	Sm.	1381·9	9·6	Jo.
8722·9	10·3	Sm.	1224·9	10·2	Jo.	1387·9	9·9	Jo.
8738·8	10·3	Sm.	1226·0	10·2	Jo.	1388·9	9·9	Jo.
8739·9	10·3	Sm.	2431233·0	10·2	Jo.	1398·9	10·2	Bt.

TABLE II

Observed Maxima and Minima of V 380 *Scorpii*

J.D. Max. 242....	Mag.	Wt.	Int. d	O−C d	J.D. Min. 242....	Mag.	Wt.	Int. d	O−C d
7305	9·5	3	...	− 3					
7492	9·5	1	187	− 3	7622	10·4	5	...	−6
7682	9·6	5	190	0					
7870	9·5	3	188	+ 1	8003	10·4	4	...	+1
8049	9·5	5	179	− 7					
8255	9·5	3	206	+11	8375	10·4	3	...	−2
8630	9·5	1	...	+12					
8995	9·5	2	...	+ 3					

Due to the small range the variable is not suitable for visual observing and scattering at times makes it difficult to determine the light curve accurately.

4. The elements are:

Range	9·5 to 10·5.
Maxima	J.D. 2427682 + 187·17*N* days.
Interval, maximum–minimum	54 days.

5. The light curve indicates that generally maxima are sharp, minima broad and there is a much more rapid rise than decrease. There is evidence that at times there is considerable departure from this type of variation. No mean light curve that has been tried is entirely satisfactory. It is probable that V 380 Scorpii belongs to the semi-regular class of variables (AF Cygni type) rather than to the long period class.

6. The star CoD −30° 13622 was not used, after the first few observations, as a comparison star. It is suspected of variability. Although the evidence is so far inconclusive, the star is generally half a magnitude fainter than its adopted magnitude of 10·62.

Whangarei, New Zealand:
1944 *December* 30.

OCCULTATIONS OBSERVED AT TEDDINGTON DURING 1943

John L. Haughton

(Received 1945 January 29)

Seven occultations were observed during 1943. All were disappearances, they were timed as on previous occasions and the results are given in Table I. The reductions were kindly undertaken by the Nautical Almanac Office, and are given in Table II. No correction has been added to the time in the reduction of the observations.

TABLE I

No.	Date	Star	Mag.	Ph.	U.T.	P.E.	Remarks
					h m s	s	
164	Jan. 14	μ Ceti	4·4	D	19 42 45·4	±0·3	
165	Jan. 15	f Tauri	4·3	D	17 37 16·1	0·4	
166	Feb. 12	179 B. Tauri	6·0	D	19 24 30·0	1·1	See note.
167	Mar. 14	BD +18° 1214	6·9	D	22 04 43·5	0·4	
168	Mar. 17	o^1 Cancri	5·2	D	22 42 43·9	0·3	
169	Mar. 17	o^2 Cancri	5·6	D	23 01 58·9	0·3	
170	Dec. 4	ψ^1 Aquarii	4·5	D	18 08 47·9	0·6	

Note.—No. 166. A very difficult observation. Discarded.

TABLE II

No.	p	q	p^2	pq	q^2	$\Delta\sigma$	$p\Delta\sigma$	$q\Delta\sigma$
164	+99	+17	97	+17	3	−0·7	−0·7	−0·1
165	+97	−24	94	−23	6	−0·5	−0·5	+0·1
167	+99	−14	98	−14	2	+0·4	+0·4	−0·1
168	+95	−32	90	−30	10	−0·1	−0·1	0·0
169	+59	+81	35	+48	65	+0·8	+0·5	+0·6
170	+94	−34	88	−32	12	−0·2	−0·2	+0·1

Teddington, Middlesex:
1945 *January* 29.

Professor E. A. Milne, M.B.E., M.A., D.Sc., F.R.S.,
President, 1943-45.